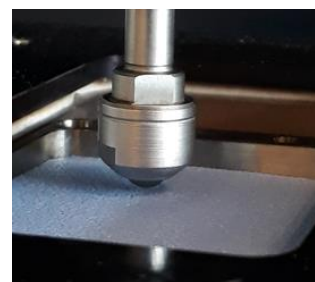


Internship Report

Tribology of simple and complex (food) systems

Effect of sample, material and operation parameters in tribological measurements with
Bruker UMT TriboLab



J. M. H. Weijgertze

NIZO food research
Utrecht University

Under supervision of:

R. H. Tromp

October 2020

ABSTRACT

Tribology is the study of friction, lubrication and wear of interacting surfaces in relative movement. Since the oral cavity is effectively a lubricated system, tribology is seen as a valuable means of relating instrumentally measured friction with oral lubrication and accompanying textural sensory attributes of food. In this work, the effects of several sample, material and operational parameters on the tribological characterization with UMT TriboLab are investigated. Simple glycerol/water mixtures confirm the effect of increasing viscosity on the lubricated friction, shifting the lubrication from the boundary to the hydrodynamic regime. Measurements of these mixtures with steel-glass, steel-rubber and PDMS-glass tribopairs in addition to the standard PDMS-rubber tribopairs show that the stiffer and smoother tribopairs generate lowered friction coefficients and a less extended mixed regime. Steel-glass tribopairs generally weaken the dependence of the friction coefficient on the entrainment speed and sample viscosity. Contact areas between PDMS probes and rubber substrates could be estimated from wear marks on PDMS probes after a measurement, and showed a linear dependence on the applied normal load. With the current tribological setup, no significant differences in friction between milks of different fat content (with saliva) could be measured. The experiments with milk and with saliva and astringent mixtures suggest that the choice of the type of tribopairs and the sliding speed are vital for a proper functionality of the UMT TriboLab for oral tribology.

TABLE OF CONTENTS

1	Introduction	4
1.1	What is tribology?.....	4
1.2	The Stribeck curve.....	4
1.3	Oral tribology.....	5
1.4	Aim	8
2	Materials and methods	9
2.1	Materials	9
2.2	Sample preparation	9
2.3	Viscosity	10
2.4	Tribological measurements.....	10
2.5	Elastic deformation of rubber probes and substrates	11
2.6	Data analysis	11
2.7	Microscopy	12
3	Results and discussion	13
3.1	Viscosity of glycerol/water mixtures	13
3.2	Effect of sample, material and operation parameters with UMT TriboLab	13
3.2.1	Viscosity	13
3.2.2	Tribopair materials	14
3.2.3	Load force.....	16
3.2.4	Particles.....	18
3.2.5	Substrate roughness.....	19
3.3	Viscosity of milk and saliva mixtures	21
3.4	Tribology of milk, saliva and astringent mixtures	21
3.4.1	Milk mixtures.....	21
3.4.2	Saliva and astringents.....	22
4	Conclusions	25
5	Outlook.....	26
	Acknowledgements.....	27
	References	28
	Appendices.....	30
	Appendix A. Data analysis.....	30
	Appendix B. Stribeck curves different tribopairs.....	32
	Appendix C. Wear	33
	Appendix D. Friction force	36
	Appendix E. Load variations.....	38
	Appendix F. Contact area measurements.....	42
	Appendix G. Glass microspheres	43
	Appendix H. Rough substrates	44
	Appendix I. Viscosity of milk, saliva and astringent mixtures	45
	Appendix J. Additional Stribeck curves milk / saliva.....	46
	Appendix K. Additional friction curves saliva.....	47

1 INTRODUCTION

1.1 WHAT IS TRIBOLOGY?

Tribology is the study of friction, lubrication and wear of interacting surfaces in relative motion.¹ The word tribology comes from the classic Greek word 'tribein', which means 'to rub'. When two surfaces are rubbed against each other, a friction force arises which opposes their relative motion and causes wear of the surfaces. A lubricant (usually a fluid) has the ability to reduce the friction and protect against wear.² The application of lubricants to reduce friction between moving surfaces dates back to ancient times, but especially in the more recent past, tribology has proved to be vital in nearly all areas of mechanical engineering. It is extensively used in engines, gear assemblies and (rolling) bearings.³ More recently, it has been recognized that tribology also plays an important role in oral processing of food.⁴

A schematic representation of a tribological contact is given in Figure 1. An upper surface moves with velocity v over a lower surface with a lubricant in between, whereby the upper surface is pushed with a normal load force F_z on the lower surface. The applied force gives rise to a friction force F_f opposite to the direction of movement. A key parameter to quantify the friction between the surfaces is the Coefficient of Friction (CoF). The CoF is defined by the ratio of the friction force to the normal load force (F_f / F_z).² The CoF depends on the surface properties (e.g. roughness), surface load, sliding speed and lubricant properties (e.g. viscosity).⁴

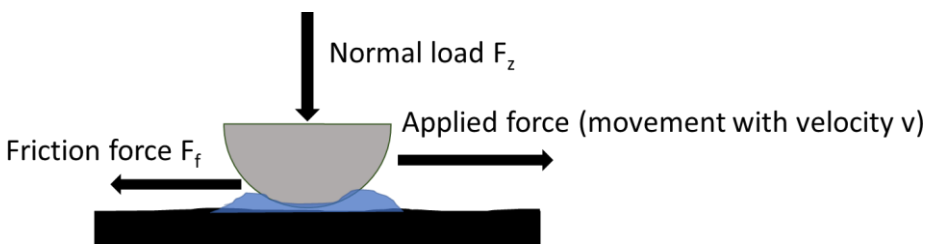


Figure 1. Illustration of two surfaces in relative motion with a lubricant (blue) in between. The upper surface pushes with a normal load F_z on the lower surface. The applied force gives rise to a friction force F_f opposite to the direction of movement. The Coefficient of Friction is defined by F_f / F_z .

1.2 THE STRIBECK CURVE

The lubrication behavior in a tribological system is commonly represented in a Stribeck curve (Figure 2). In a Stribeck curve, the CoF is traditionally plotted against the dimensionless Hersey number: $n*\mu/p$, where n is the rotational speed in nr of revolutions per unit time, μ the dynamic viscosity of the lubricant and p the normal load per contact area.⁵ The Hersey number was originally defined for lubrication in journal bearings, and is not directly applicable to all other tribological systems. Therefore, variations on the Hersey number such as entrainment speed $[m/s] * \text{viscosity} [Pa\cdot s] / \text{load} [N]$ are used as well. In (geometrically) similar systems that are similarly loaded and lubricated, the CoF only depends on the Hersey number. The thickness of the lubricant film in the tribological contact correlates with the Hersey number. The extent of fluid entrainment into the contact increases with entrainment speed and viscosity.⁶

Three lubrication regimes can be distinguished in the Stribeck curve. The first is the boundary regime, which usually occurs at low speeds. There is no fluid entrainment into the contact and the friction is dominated by the surface asperities.⁷ The second is the mixed regime, where the film thickness in the contact is of similar dimension as the surface asperities, and asperity contact occurs occasionally.⁸ The fluid entrainment into the contact creates a pressure which supports the separation of the two surfaces, resulting in decreasing friction coefficients with

increasing speed. The third is the hydrodynamic regime, where the surfaces are completely separated and the load is carried by the fluid film. The friction depends on the rheological properties of the fluid in the contact. The CoF increases due to fluid drag forces.⁹

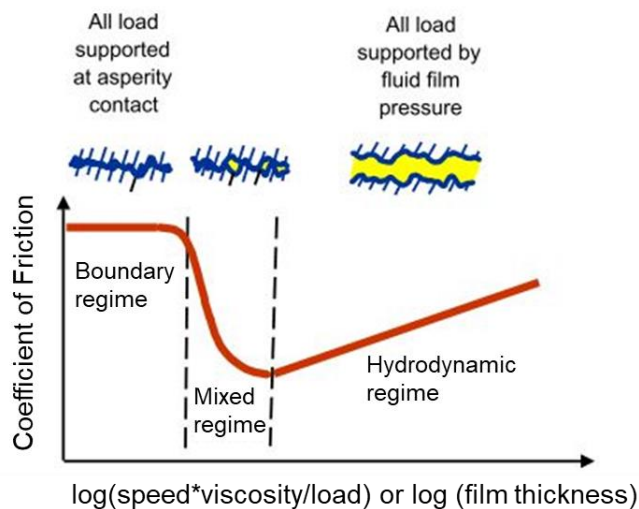


Figure 2. Schematic Stribeck curve. Adapted from ref.⁷

1.3 ORAL TRIBOLOGY

Eating and oral processing of food is a dynamic process, in which sensory perception plays an important role. The tactile texture of food is perceived with the oral apparatus.¹⁰ Several interacting surfaces are involved in the process of eating, e.g. tongue-palate and tongue-teeth. The food consumed and the saliva present in the mouth act as lubricants to these surfaces. Throughout the oral processing, the lubrication passes the different lubrication regimes in the Stribeck curve. In the first stage, bulk properties of the food or beverage are dominant and mouthfeel attributes are best described by rheology (Figure 3). The lubrication is in the hydrodynamic regime. When the product is broken down to a thinner film, the interactions between the surfaces in the mouth with the food film become important and the lubrication is in the mixed or boundary regime.^{7,9} The type of food determines which lubrication regime is dominant; e.g. the lubrication of thicker fluids will be more governed by the hydrodynamic regime than the lubrication of less viscous fluids, where a thin film is more easily formed.⁹

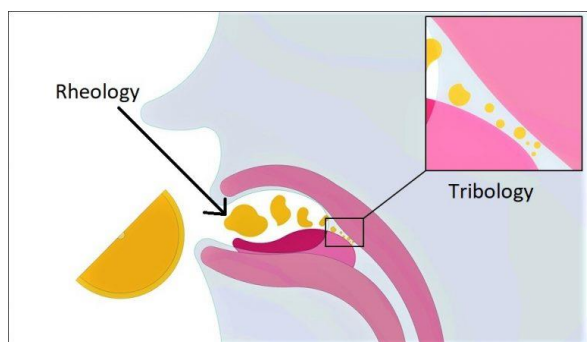


Figure 3. Stages of oral processing. First, the perceived food texture is best described by rheology. When the food is broken down, the frictional properties between the food and the oral surfaces become essential, and this is best described by tribology. Reprinted from ref.¹¹

Textural properties

The texture of food can be described using a whole range of mouthfeel attributes, such as softness, springiness, thickness, brittleness, roughness, astringency and creaminess.¹⁰ Throughout the oral processing, the intensity of perception of the sensory features varies, depending on the lubrication regime in which they are dominant. Attributes may be linked more to rheology, more to tribology or to a combination of both. Already in the previous century, Kokini proposed a model based on the tongue-palate interaction linking the friction coefficient (tribology) and / or the fluid viscosity (rheology) to three main sensory attributes: thickness, smoothness and slipperiness.¹² He found that thickness is closely related to viscosity, while the perception of smoothness is purely dependent on the lubrication properties (friction) of the food in the oral cavity. Slipperiness could be correlated with the reciprocal of the sum of the viscous and the friction force. The finding that textural sensory features can be correlated with instrumentally measurable parameters is crucial to the way of testing food quality. Traditionally, the food quality is measured using a sensory panel that assesses the food on the basis of particular sensory features. The potential of using tribology for instrumental prediction of food texture properties is more convenient in terms of time saving and objectivity.¹⁰

Creaminess

A principal sensation in the oral perception of dairy products is creaminess. Creaminess is a complex sensation related to the fat content of a product and is associated with attributes like smoothness, thickness, taste and aroma. The opposite of creaminess is a feeling of roughness.¹³ In terms of tribology, an increased perception of creaminess is related to a decreased friction coefficient.¹⁴ This is ascribed to the coalescence of fat droplets under shear. Dairy products such as milk are essentially emulsions of fat globules in an aqueous phase.¹⁵ Emulsions that are more sensitive to coalescence, give rise to the highest creaminess and lowest friction.¹⁶ The presence of smaller and more numerous fat droplets instead of larger and lesser droplets results in a higher creamy mouthfeel.¹³

Astringency

Another common mouthfeel attribute is astringency, which is perceived in many types food, such as red wine and tea. It is described as a roughening, puckering and drying-out mouthfeel, linked to an increase in oral friction.¹⁷ Astringency is mostly described as a physical perception, related to a loss in oral salivary lubrication. To explain possible mechanisms behind the sensation of astringency, it is useful to consider the lubrication of saliva in general. It is known that saliva itself is a good lubricant, which is verified in tribological measurements.¹⁸ The lubricating ability of saliva is normally ascribed to the mucins that are naturally present in saliva. Mucins are glycoproteins that play a part in protecting oral surfaces against degradation and protect against microbes.¹⁹ Mucins can act as a aqueous boundary lubricant: they form a brush-like layer on the soft surfaces in the mouth, entrapping water in a hydration layer, and so keep the friction low. However, the exact lubrication mechanism of saliva is not known, as the presence of only highly glycosylated mucins in artificial saliva cannot reproduce the lubricating properties of real saliva.¹⁸

The sensation of astringency is usually linked to the binding of astringent species (often polyphenols) to salivary proteins (Figure 4).²⁰ The precipitation of such protein-polyphenol aggregates may lead to the loss in salivary lubrication, possibly via a decrease in the viscosity of the salivary film or by the direct increase in the perception of roughness caused by the precipitates.¹³ However, astringency cannot always be correlated to altered lubrication in tribological experiments.²¹ Hence, it is believed that other mechanisms might play a role in the perception of astringency as well. Astringent species or precipitates might disrupt the salivary film and directly affect the salivary pellicle beneath, causing an astringent mouthfeel. Even the interaction of astringent species with receptors in the mouth is proposed as a contributing factor

in the perception of astringency.^{17,20} This would mean that astringency is not purely a physical tactile sensation, but also a chemical perception.

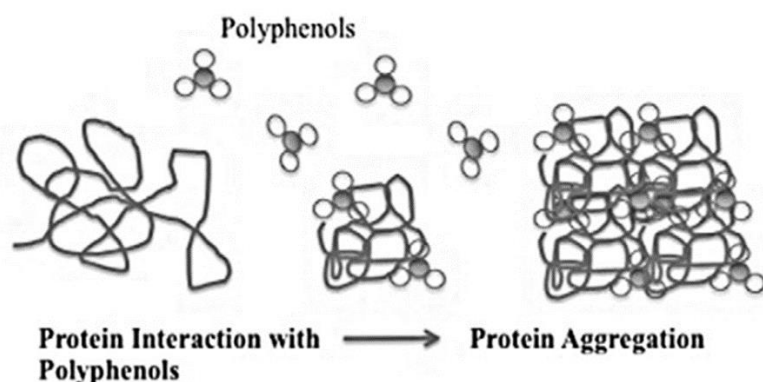


Figure 4. Classical model of the mechanism behind astringency. Reprinted from ref.²⁰

As already mentioned, polyphenolic molecules often give rise to astringency. Common classes of polyphenols are tannins and catechins that are present in wine or tea. It has been proved that such molecules easily form complexes with salivary proteins, probably through hydrophobic interactions and the formation of hydrogen bonds.²⁰ In tribological measurements with saliva, tannic acid, catechin and red wines, positive correlations between the friction coefficient and the perceived astringency have been found.²² Other astringent compounds include metal alums and acids.²⁰ In addition, the protein lysozyme (occurring in hen egg white) is able to precipitate salivary proteins (mostly acidic ones, since lysozyme is rich in basic amino acids).²³ Upadhyay et al.²⁴ found that adding artificial saliva to lysozyme-stabilized emulsions generally led to increased or similar friction coefficients, while adding saliva to emulsions stabilized by whey protein isolate clearly resulted in lowered friction.

Particles

The presence of particles in food can have a large effect on the perceived texture. Common food-particles include starch and various protein types. Particles can give rise to a gritty or grainy mouthfeel and a reduced smoothness, as was found for microcrystalline cellulose²⁵ (6-80 μm) and acid milk gel particles²⁶ (50-480 μm), with larger particles having a more severe effect. In general, larger particles and sharper particle shapes cause a higher rough after-feel and astringent lip feel.¹³ These oral perceptions can also be related to friction. Laiho et al.²⁷ found that with (fat-free) yoghurts, larger particle sizes could be correlated to a higher friction coefficient and an increased grainy mouthfeel. Liu et al. explained the increasing friction coefficient with increasing concentration rice starch particles (5 μm) in dispersion by the indirect surface roughening due to the irregular shape of the rice starch.²⁸ On the other hand, smooth, spherical particles can cause a decrease in friction coefficient by a mechanism called the ball-bearing effect, which exploits the fact that rolling balls have a lower friction than sliding surfaces. It is for example observed in nanoparticle addition to common lubrication oils,²⁹ but also for aqueous dispersions of microparticulated whey protein (MWP).³⁰

Surfaces

In tribological measurements connected with oral tribology, the most commonly used surface to date is polydimethylsiloxane (PDMS). It is considered as a feasible surface as it can have a close resemblance to the elasticity of the human tongue.¹⁰ It is often used in combination with a steel ball to mimic the contact between the soft tongue and the hard palate. However, in common tribological setups this can give rise to contact pressures substantially higher than in the oral cavity.¹⁸ Therefore, the use of soft contacts (rubber-rubber) and /or low contact pressures (of

the order of 0.1 N) could more closely resemble the in-mouth conditions. As opposed to the most PDMS surfaces used, the tongue is not a smooth surface but is covered with various papillae (of sizes in the order of 100 μm) giving the tongue some roughness. To imitate this, Ranc et al.³¹ used PDMS substrates covered with hemispherical pillars in the same dimensions as the tongue papillae. Krzeminski et al. used rubbers with different surface morphologies to cover the different roughness scales of the human tongue.³² They found that the lubrication properties of oil, water and semi-solid milk products are highly dependent on the surface morphology and roughness. Moreover, whey protein isolate gel is recommended as a tribological surface, because its hydrophilicity and elasticity are similar to that of the tongue. Using WPI gel, Di Cicco et al.³³ achieved a better distinction in friction between several types of yoghurt than with a PDMS surfaces. Pig's tongues can also be used as surface for food tribology,³⁴ which might seem convenient since it will most closely resemble the human's tongue. However, pig's tongues suffer from fast degradation, lack of uniformity and limited availability, which complicates their use.

1.4 AIM

In this study, tribological experiments are performed with Bruker's UMT TriboLab. On the basis of a standard measurement protocol, the effect of several sample, material and operation parameters on the resulting friction is investigated. Glycerol/water lubricated systems are used to explore the influence of sample viscosity, tribopair materials (rubber, steel, glass), normal load force, particle addition and substrate roughness on the tribological characterization. Additionally, experiments with milks of different fat content, with saliva, and with the representative astringent substances tannic acid and lysozyme were conducted to find out to which extent the UMT TriboLab is able to distinguish the properties of these food(-related) products with the available PDMS-rubber and steel-glass tribological setups. This should eventually lead to a better understanding of the relation between friction and mouthfeel and especially of the functionality of the UMT TriboLab in food tribology.

2 MATERIALS AND METHODS

2.1 MATERIALS

Glycerol (99.5%, Scharlau), glass microspheres (sieve fractions: 20-30 μm and 45-53 μm , Whitehouse Scientific), rhodamine B (for fluorescence, Sigma-Aldrich), mucin (from porcine stomach Type III, Sigma-Aldrich), NaCl (for analysis, Merck KGaA), K_2HPO_4 (anhydrous for analysis, Merck KGaA), $\text{Na}_2\text{CO}_3 \cdot 10\text{H}_2\text{O}$ (reagent grade, Scharlau), HCl (37%, Scharlau), NaOH (pellets, reagent grade, Scharlau), lysozyme (from chicken egg white, lyophilized powder, protein >90%, Sigma-Aldrich), tannic acid (ACS reagent, Sigma-Aldrich), sunflower oil (AH private label), skim milk (pasteurized, 0% fat, AH private label), whole milk (pasteurized, 3.5% fat, AH private label) were used as received. RO water was used in all experiments.

2.2 SAMPLE PREPARATION

Several non-food and food-related samples were prepared for tribology experiments.

Glycerol/water mixtures were prepared in 100/0, 90/10, 80/20, 70/30, 60/40 and 50/50 w/w%. Gw5050, gw8020 and glycerol were also prepared with 5 wt% glass microspheres added (20-30 μm and 45-53 μm).

Artificial saliva was produced by adding 2 wt% of mucin to a standard salt solution containing 1.5 g/L NaCl, 1.5 g/L K_2HPO_4 and 0.5 g/L Na_2CO_3 which was set at pH 6.7 by addition of HCl and NaOH. The saliva was added in 5 wt% to skim milk, whole milk and skim milk/whole milk 50/50 w/w% to mimic the in-vivo oral situation during beverage processing. Also, only salt solution was added in 5 wt% to the mentioned milk samples as a reference.

To probe the effect of the presence of an astringent in a solution, lysozyme and tannic acid were added in 2 wt% to saliva with mucin and the standard salt solution. These solutions were added in 5 wt% to skim milk.

See Table 1 for an overview of the prepared mixtures and their nomenclature used throughout this report.

Table 1. Samples for tribology experiments and their nomenclature.

Sample composition	Label
Glycerol/water 50/50 – 90/10 w/w%	gw5050 – gw9010
Standard salt solution for saliva	salt solution
Artificial saliva (with mucin)	salivam
Skim milk	mfat0
Whole milk	mfat100
Skim milk / whole milk 50/50 w/w%	mfat50
Milk with 5 wt% salt solution	mfat..-s
Milk with 5 wt% salivam	mfat..-sm
Salt solution with 2 wt% lysozyme or tannic acid	s-lys or s-tan
Salivam with 2wt% lysozyme or tannic acid	sm-lys or sm-tan
Skim milk with salt solution with lysozyme	mfat0-s-lys
Skim milk with salt solution with tannic acid	mfat0-s-tan
Skim milk with salivam with lysozyme	mfat0-sm-lys
Skim milk with saliva and tannic acid	mfat0-sm-tan

2.3 VISCOSITY

The viscosity of glycerol/water mixtures was measured at 22 °C with a rheometer (AR-G2, Waters TA Instruments) with concentric double gap cylinder geometry. The shear rate was increased from 1 s⁻¹ to 1000 s⁻¹ while recording ten data points per decade.

The viscosity of milk, salivam and salt solution samples was measured at 22 °C with a viscometer (Rolling-ball viscometer Lovis 2000 M/ME, Anton Paar) with a \varnothing 1.59 mm capillary and a 1.5 mm steel ball of density 7.70 g/cm³. The viscosity of each sample was averaged over three consecutive measurements.

2.4 TRIBOLOGICAL MEASUREMENTS

Tribological measurements were performed with an UMT TriboLab (Bruker Nano, Inc) equipped with a fast reciprocating (oscillating) linear drive (rec drive, horizontal motion over a stroke length of 25 mm). 0.18 mL of sample was sheared between an upper surface consisting of a semi-spherical PDMS probe (d=5 mm) or a stainless steel ball (d=8 mm) in a ball holder and a lower flat surface (substrate) of custom-made silicone rubber or glass (Thermo Scientific Menzel- Gläser microscope slide, cut to fit the rec drive). Figure 5 shows the setup of a typical measurement. Each measurement, a new PDMS probe and a new position on the rubber substrate or a new rubber substrate were used, because the rubber wears down during a measurement. For all measurements with steel and glass, the same probe and substrate were used.

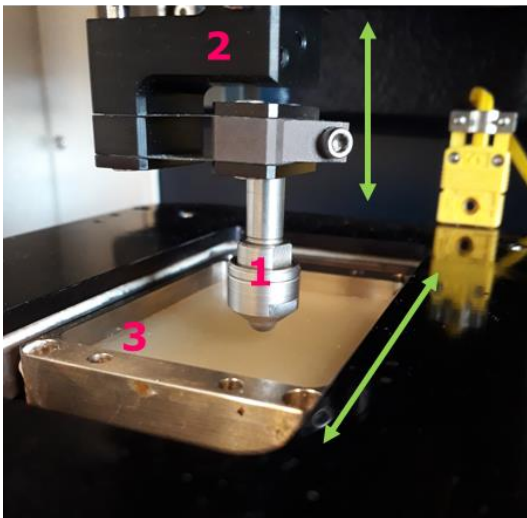


Figure 5. Measurement setup of the UMT Tribolab. 1. The ball holder containing the upper surface (the probe). 2. The carriage, in which the ball holder is mounted. The carriage regulates the vertical (Z-direction) movement of the ball holder. 3. The reciprocating drive containing the bottom surface (substrate). Arrows indicate the directions of movement of the carriage and the reciprocating drive.

Preparation of the PDMS (polydimethylsiloxane) probes is described in Stee et al.³⁵ In addition, rough substrates were fabricated from Rapid putty Non Food. For this, two types (blue and white) rubber putty were mixed in equal parts and molded on sandpaper (SandBlaster 3M grit sizes P400, P180, P120 and P80) to produce different roughnesses, and on a petri-dish to obtain a smooth reference substrate.

For all measurements, a standard test script was used comprising nine steps of ascending speed (0.1, 0.25, 0.5, 0.75, 1.0, 1.25, 1.5, 1.75 and 2 Hz) with ten oscillations per step. Data was collected with time intervals of 0.005 sec. Each test was operated in the load controlled mode at a constant load (0.2 N – 4 N). Measurements were repeated at least two or three times.

2.5 ELASTIC DEFORMATION OF RUBBER PROBES AND SUBSTRATES

The stiffness of the PDMS probes and rubber substrates was measured using an electromechanical testing system (Instron 5543). A disk of rubber substrate or a cylindrically cut PDMS probe was compressed while monitoring the stress (force / area) and the strain (Δ length / total length). The Young's modulus was calculated from a linear (elastic) part of the stress-strain curve; for the PDMS probes between 0.1 and 0.3 mm/mm and for the rubber substrates between 0.12 and 0.3 mm/mm. The measurement was performed on five different PDMS probes and rubber substrates.

2.6 DATA ANALYSIS

The raw data output of the tribometer was used for data analysis, with as main goal the construction of Stribeck curves of the measurements. Parameters saved in the raw data files and used in the analysis include the normal load (force in the z-direction with which the probe touches the substrate), the friction force, the position of the reciprocating drive (LVDT, horizontal motion) and the carriage height (vertical position of the ball holder). The data was available with a time resolution of 0.005 sec (starting again at 0.000 sec at every step).

For the data-analysis, a custom-written MATLAB script was used. Using the LVDT values and the time intervals, the velocity of the rec drive over the course of the experiment was calculated. CoFs were calculated by dividing all separate friction force data points by the corresponding normal load data points. A cubic smoothing spline was fitted to the time and velocity data to discard the measurement noise. For an example of the effect of smoothing, see Figure A 1 in Appendix A. Furthermore, it was noted that at the beginning of each step the rec drive was still in transition from the previous step to the current step, such that in the first oscillation the maximum speed achievable for the current frequency was not yet reached. Therefore, the data in the first 2 / Hz second of each step was rejected. An example of this time clipping is shown in Figure A 2.

From the thus obtained data, an average CoF value per step could be calculated. The CoF is best calculated where the acceleration is zero, i.e. at the maximum speed of each stroke, since there purely friction force is measured. In this regard, the data (both speed and CoF) was selected based on the criterion that speeds should be maximally 5% below the maximum speed (so when the maximum speed in a step is 40 mm/s, speeds from 38 mm/s to 40 mm/s are allowed). In addition, the data was selected to fall within 4 mm deviation from the middle position of the rec drive (where the maximum speed is reached) to discard any outliers. The resulting speeds and CoFs were averaged per step, yielding a series of nine CoF values as function of speed. Since there is a backward and forward direction involved in the movement of the rec drive, positive and negative velocities and corresponding CoFs can also be treated separately. The CoFs obtained for positive and negative velocity were generally not exactly equal (however, neither of the directions gives more often higher CoFs).

When instead of the CoF only the friction force was used as output, an extra selection criterion was applied where only data within 5% deviation from the set normal load was retained. When reporting CoFs, such a selection is not required since the division of the friction force by the normal load already compensates for possible variations in the normal load force.

For each step, the parameter $\text{Speed} \cdot \text{Viscosity} / \text{Load}$ was calculated in addition to the pure speed. For this, all speed data points (selected as explained above) were divided by the corresponding normal load data points, and multiplied with a chosen viscosity value (of the sample which data is analyzed). This parameter is similar to the dimensionless Hersey number,⁵ except that here a length is missing. This missing length might be related to the contact area and gap size between the surfaces in relative movement.

Eventually, per measurement a series of nine CoFs or friction forces and corresponding speeds, $\text{Speed} \cdot \text{Viscosity} / \text{Loads}$ and normal loads was obtained. The final data points were calculated by averaging over three (or sometimes two) measurements. In some cases, a cubic smoothing

spline interpolation was applied to data of multiple measurements with lubricants of different viscosity (giving different Speed*Viscosity/Load values).

Another manner to calculate CoFs as a function of speed from the data of a tribological experiment with UMT TriboLab, is using the Oscil.COF option in the UMT Viewer software. An explanation of this data analysis method and a comparison to the raw data analysis can be found in Appendix A2.

2.7 MICROSCOPY

PDMS probes and (rough) rubber substrates before and / or after use in a tribology experiment were imaged using a stereomicroscope (Leica MZ16, camera: Leica MC 170HD).

Glass microspheres as well as salivam mixtures with tannic acid and lysozyme were imaged with an optical microscope (Leica Reichert-Jung Polyvar, camera: Leica MC 120HD).

A Confocal Laser Scanning Microscope (CLSM, Leica TCS SP5) was used to visualize track formation on silicone rubber substrates after a tribology experiment. To this end, a drop of 1 wt% rhodamine B solution in water was put on the track on the rubber substrate. A 543 nm HeNe laser was used for excitation of the rhodamine B dye.

3 RESULTS AND DISCUSSION

Tribological experiments with glycerol/water mixtures were carried out to explore the effects of viscosity, tribopair materials, load force during a measurement, presence of particles in a sample and substrate roughness on the friction. Additionally, the tribological properties of milk, saliva and astringent mixtures were investigated using a standard test procedure on the UMT TriboLab.

3.1 VISCOSITY OF GLYCEROL/WATER MIXTURES

The viscosity of glycerol/water mixtures ranging from pure glycerol to 50/50 w/w% is presented in Figure 6a. Figure 6b shows the viscosities of these mixtures as a function of shear rate. The viscosity increases with the fraction of glycerol in the mixture. Sunflower oil has a viscosity similar to gw8020 (Figure 6c). All fluids show Newtonian behavior.

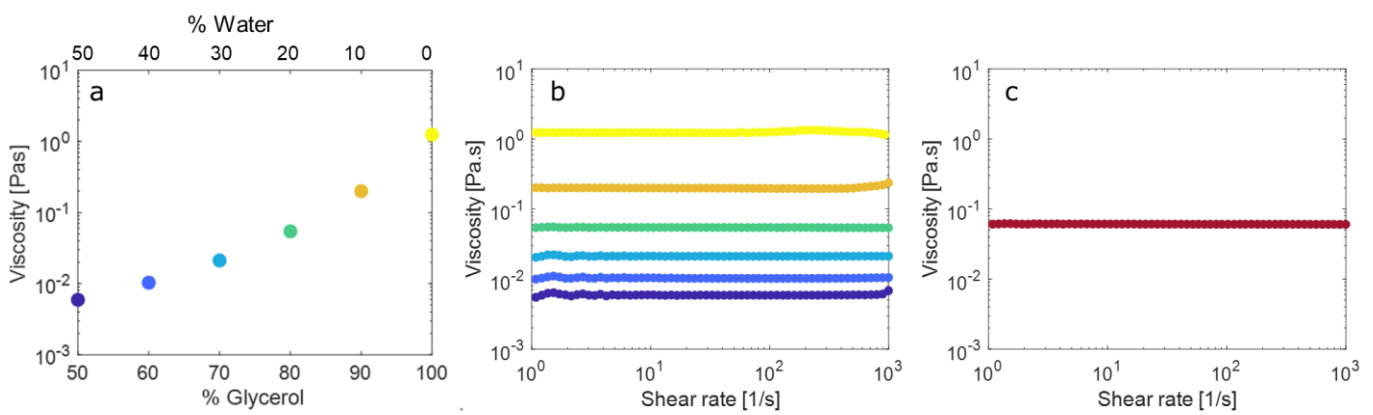


Figure 6. Viscosity of glycerol/water mixtures as a function of (a) mixture composition in w/w% and (b) shear rate. The viscosities reported in (a) are the averages over the data points shown for each mixture in (b). The standard deviation falls within the marker size. The colors in (b) correspond to the same mixture as the colors in (a). (c) Viscosity of sunflower oil. All fluids show Newtonian behavior.

3.2 EFFECT OF SAMPLE, MATERIAL AND OPERATION PARAMETERS WITH UMT TRIBOLAB

3.2.1 Viscosity

To investigate the effect of viscosity on the CoF measured with UMT TriboLab, tribological measurements with six glycerol/water mixtures (gw5050 – glycerol) were carried out. Figure 7 shows the obtained CoFs for all mixtures as a function of Speed*Viscosity/Load. The individual curves together form a master Stribeck curve. This points out that the change in CoF is only dependent on the sample viscosity and the entrainment speed, as might be expected for lubricants with the same substance properties (e.g. same polarity). Glycerol and water are both simple hydrophilic fluids.³⁶

Mixtures with higher water content and thus lower viscosity are in the boundary and mixed regime of the Stribeck curve, while mixtures with higher glycerol content are in the transition region from the mixed to the hydrodynamic regime. Pure glycerol is in the hydrodynamic regime, where the load is fully carried by the fluid.

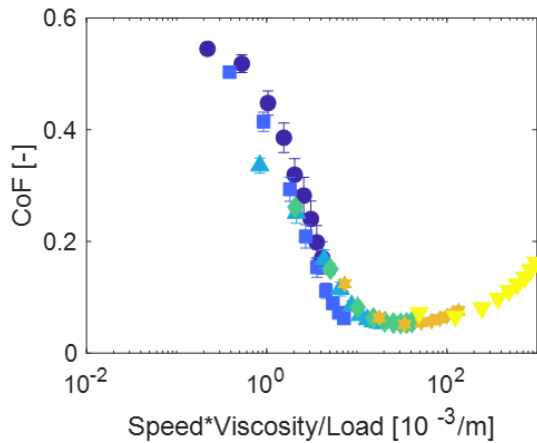


Figure 7. Stribeck curve of glycerol/water mixtures measured at 0.2 N normal load with PDMS-rubber tribopairs. ● = gw5050, ■ = gw6040, ▲ = gw7030, ◆ = gw8020, ★ = gw9010, ▼ = glycerol. Standard deviation is indicated by error bars.

3.2.2 Tribopair materials

The effect of using different tribopair materials (i.e. the surfaces in between which the fluid is sheared) on the friction was investigated by conducting tribological experiments with all glycerol/water mixtures using four different tribopair combinations. The used tribopairs are PDMS-rubber, PDMS-glass, steel-rubber and steel-glass, where PDMS and steel are the upper surfaces and rubber and glass the bottom surfaces.

An important characteristic of the materials is their stiffness, which informs on how easily a material can be deformed. A measure for the stiffness of a material in the region where it responds elastically to an applied pressure is Young's modulus.³⁷ A high Young's modulus means that a large pressure is needed to deform the material only a little. The Young's moduli for a PDMS probe and a rubber substrate measured by a compressive test are 3.1 ± 0.1 MPa and 4.4 ± 0.2 MPa respectively. A PDMS probe is thus a little softer than a rubber substrate. For glass and stainless steel, Young's moduli of 50-90 GPa and 180 GPa are reported, respectively.³⁸ This shows that PDMS and rubber are much softer materials than glass and steel. These differences might have an influence on the tribological measurements.

Figure 8 presents the Stribeck curves of the glycerol/water mixtures measured between the four tribopairs at 0.2 N normal load. At the low speeds and viscosities, there is a clear distinction between the curves, with PDMS-rubber giving the highest CoFs and steel-glass the lowest. Interestingly, the order in which the tribopairs give higher CoFs correlates with the decrease in the stiffness and hardness and smoothness of the materials. PDMS probes give a higher friction than the steel probe and the rubber substrates gives a higher friction than the glass substrate. Intuitively, it is logical that smoother materials give lower friction. The order of the Stribeck curves is preserved when measuring at another normal load (see Figure A 4 in Appendix B).

The difference in CoFs could more particularly be related to the lubrication regime accessed by the tribopairs. PDMS-rubber gives the full mixed regime, from the transition boundary-mixed regime to the beginning of the hydrodynamic regime. In contrast, steel-glass only gives the transition of the mixed to the hydrodynamic regime and the beginning of the hydrodynamic regime. In general, friction coefficients are the lowest in the transition from the mixed to the hydrodynamic regime, since there the influence of the asperities disappears and the drag force is still minimal. The absence of the boundary regime and most of the mixed regime for steel-glass could be explained by the smoothness and stiffness of these materials, giving minimum contact area and asperity contact. Larger deformation and less smoothness of the rubber tribopairs could cause the surface asperities to have more effect by locally reducing the smaller gap size, and thereby give a more extended mixed regime.

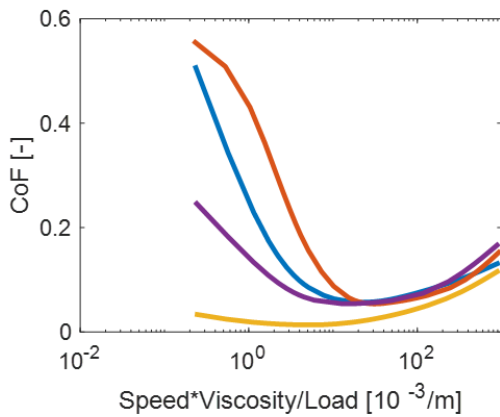


Figure 8. Stribeck curves of glycerol/water mixtures measured at 0.2 N normal load with PDMS-rubber (—), PDMS-glass (—), steel-rubber (—) and steel-glass (—) tribopairs. The curves are spline interpolations of the separate data points.

Noteworthy is the fair overlap of the Stribeck curves of all four materials at the higher speeds and viscosities. Here, the friction is in the hydrodynamic regime. The overlap of the curves shows that the fluid properties dominate in the hydrodynamic regime, while the effect of the tribopair materials diminishes.

The difference between the tribopair material properties is also expressed in the degree of wear during a measurement. PDMS probes and rubber substrates often showed clear traces of wear (a wear spot on the probe or a wear track on the substrate) after measurements with a PDMS probe on a rubber substrate. Notably, when glycerol was used as lubricant, no wear spot on the PDMS probe and no track on the substrate was observed. This underlines that lubrication with glycerol is in the hydrodynamic regime, where the load is carried completely by the fluid. The PDMS probes and rubber substrates did not show signs of wear when used in combination with the glass plate or the steel ball. A more elaborate discussion of wear during the tribological experiments can be found in Appendix C.

3.2.2.1 Wettability

Another important material characteristic is the wettability of the surface. This property is reflected in the comparison of the CoF of sunflower oil (hydrophobic) with the CoF of glycerol/water (hydrophilic) on the same surface. Figure 9 shows Stribeck curves of glycerol/water together with the curves of sunflower oil measured at 0.2 N normal load between PDMS-rubber tribopairs (a) and steel-glass tribopairs (b). Stribeck curves of glycerol/water and sunflower oil at 0.5 N and 0.9 N are shown in Figure A 5 in Appendix B.

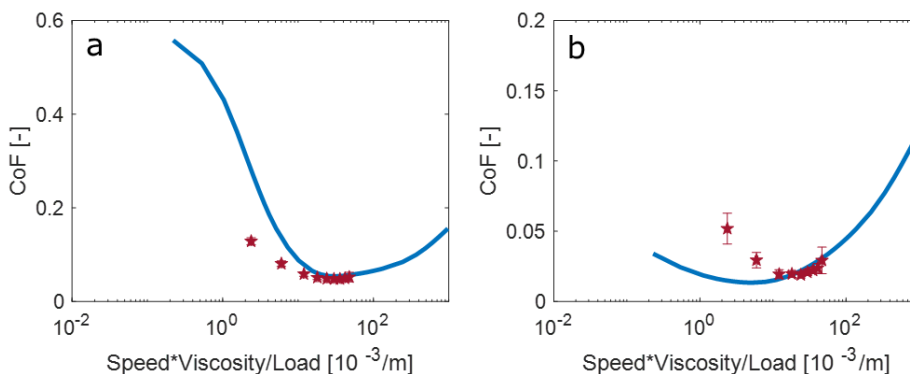


Figure 9. Stribeck curves of glycerol/water mixtures (—) and sunflower oil (★) at 0.2 N with PDMS-rubber (a) and steel-glass (b) tribopairs.

Consistently, the CoFs of sunflower oil at the lower speeds lie below the Stribeck curve of glycerol/water in the case of the PDMS-rubber surfaces and lie above the glycerol/water curve in the case of steel-glass. This can be explained by the difference in wettability between PDMS-rubber and steel-glass. The rubber is hydrophobic (as can also be seen in the images in Figure A 6 showing the difference in spreading of glycerol/water and sunflower oil on the rubber substrate), whereas glass and steel are more hydrophilic. This agrees with the observation in literature that a fluid is a better lubricant when it wets the substrate well, i.e. it gives lower CoFs in the boundary and mixed regime than a lubricant that wets the substrate poorly.³⁹ Again, we see that in the hydrodynamic regime the material characteristics are less important and the friction is mostly governed by the viscosity of the fluid.

3.2.3 Load force

To investigate the effect of the normal load during a tribological experiment on the Stribeck curves, measurements with glycerol/water mixtures at 0.2 N, 0.5 N and 0.9 N normal load force were performed. Figure 10 presents the resulting Stribeck curves for PDMS-rubber, PDMS-glass, steel-rubber and steel-glass tribopairs.

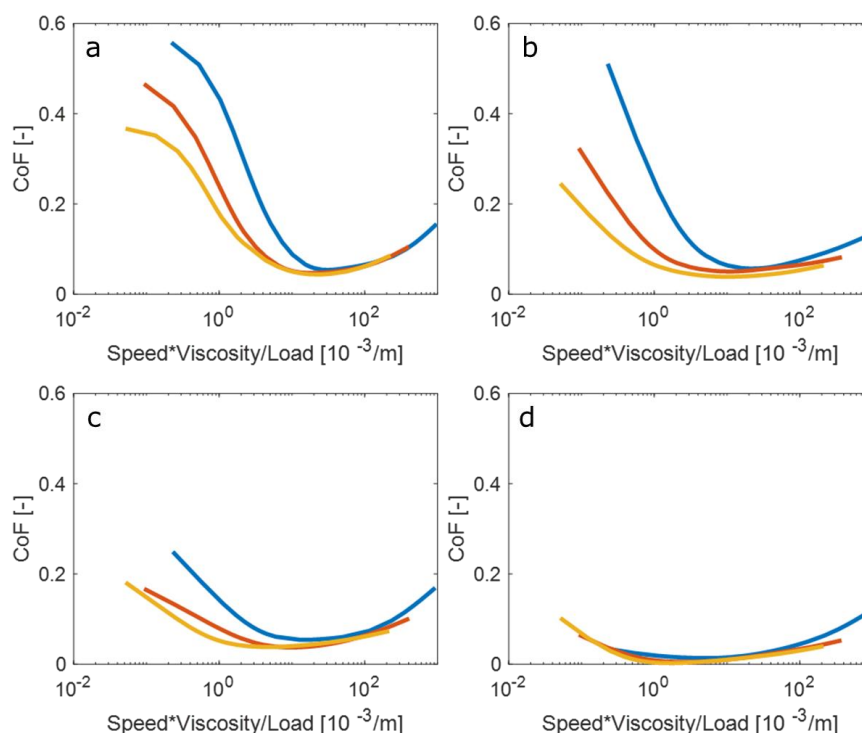


Figure 10. Stribeck curves of glycerol/water mixtures measured at 0.2 N (—), 0.5 N (—) and 0.9 N (—) normal load with PDMS-rubber (a), PDMS-glass (b), steel-rubber (c) and steel-glass (d) tribopairs. The curves are spline interpolations of data points.

The most evident observation is that friction coefficients decrease with an increase in normal load. This is an indirect result of the definition of the CoF (friction force / normal load): division by a larger load can make the CoF go down. Apparently, the substrate-lubricant system reacts in a non-linear fashion to increasing load. Appendix D looks deeper into the difference between the CoF and friction force and their dependence on the normal load.

It is interesting to note that PDMS-rubber, PDMS-glass and steel rubber (Figure 10a, b, c) display divergent CoFs for the different loads at lower speeds and viscosities. Here, the lubrication is in the mixed regime. Presumably, the difference in CoFs arises from the variation in intensity of the asperity contact between the surfaces, with more severe asperity contact for a higher load. In contrast, the Stribeck curves for steel-glass tribopairs (Figure 10d) overlap at

these speeds and viscosities. This could be explained considering the smoothness and stiffness of these materials compared to rubber. Even at the highest applied normal load, there is no significant asperity contact between the steel-glass surface and therefore the friction is hardly influenced by the load. Likewise, for all tribopairs, the CoFs at the different normal loads overlay quite well in the hydrodynamic regime, attributable to the lack of asperity contact. Especially PDMS-rubber seems to give a perfect master Stribeck curve in the hydrodynamic regime.

Finally, an observation regarding the load force worth mentioning is that during a tribological measurement, the load force applied by UMT TriboLab can oscillate slightly around the set load force (0.2 N, 0.5 N or 0.9 N in this case). The fluctuations are not enormous and were not correlated to mutual differences in CoF between multiple measurements of the same sample (Figure A 16). Moreover, the division of the friction force by the true normal load to obtain the CoF is already a sort of inherent compensation for the small fluctuations in the load force. Nevertheless, inspection of the variations in the load force can give some interesting insights into the operation mechanism of UMT TriboLab. Therefore, some further analysis of the variations in the normal load during a measurement is given in Appendix E.

3.2.3.1 Contact areas

Section 3.2.2 mentions the formation of wear spots on PDMS probes after measurements using a rubber substrate as bottom surface. It was observed that the size of the wear spots increases with the normal load, indicative of a larger probe deformation with a higher load, as expected. The size of the wear spot can be taken as reliable estimation of the contact area between the probe and the substrate. These contact areas inform on the deformation of the probes during a measurement. Contact areas between the PDMS-rubber surfaces in measurements at normal loads ranging from 0.2 N to 1.1 N (using gw6040 as a lubricant) were determined from stereomicroscopy images of the probes (Figure A 17 in Appendix F).

Interestingly, the contact area depends linearly on the applied normal load (Figure 11).

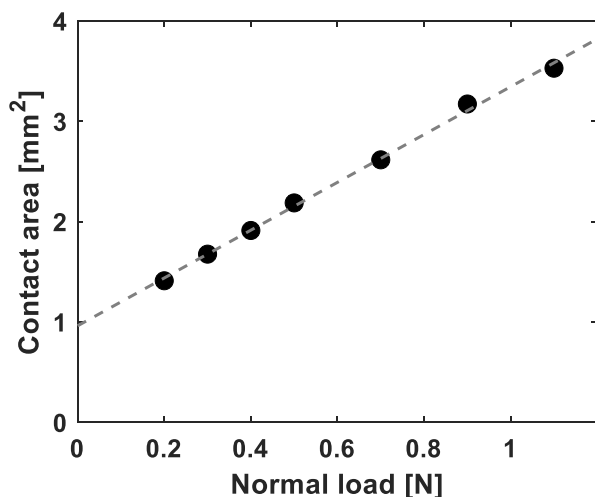


Figure 11. Contact areas between PDMS-rubber surfaces as a function of the normal load during a tribological measurement. The contact areas were determined from wear spots on PDMS probes (see Appendix F). The measured contact area is an average over at least three probes. The R^2 value of the linear fit is 0.9975.

The contact areas can be related to deformation lengths (length that a PDMS probe decreases in the z-direction when a load is applied on it) by approximating the contact area as the base area A of a spherical cap and the deformation length as the height h of the cap. In this model, it is assumed that there is no equatorial expansion of the PDMS probe, and that the substrate does not deform (which is reasonable since the substrate is stiffer than the probe, section 3.2.2). A

and h are related via $A = 2nrh$, where r is the sphere radius. Hence, the linear relation between the contact area and the normal load implies also a linear relation between the deformation length and the normal load. This is in fact what is stated by Hooke's law for small elastic deformations.³⁷ The square root of the contact area defined here could be used to calculate the dimensionless Hersey number.

Remarkably, extrapolation to zero normal load gives a contact area larger than zero. This is possible when the probe still touches the substrate when the TriboLab detects a normal load of 0 N. It was tested whether this could be true by performing a measurement at 0 N normal load. Indeed, a small wear spot on the PDMS probe was observed after this measurement (Figure A 18). This corroborates the finding that the friction force would not be zero at zero normal load (Figure A 11).

3.2.4 Particles

The effect that particles can have on the friction was investigated by performing measurements with glycerol/water mixtures to which glass microspheres of 20-30 μm or 45-53 μm had been added. Microscopy images of the particles can be found in Figure A 19 in Appendix G. Figure 12 presents the Stribeck curves of glycerol/water-particles lubricated systems together with curves of purely glycerol/water. Some features in the curves measured at 0.2 N normal load for both particle sizes (Figure 12a, c) stand out: the CoF of particle-lubricated systems is lowered near the boundary regime w.r.t. the mixtures without particles, and there is a plateau present in the Stribeck curve at intermediate speeds and viscosities, especially with the 45-53 μm particles. On the contrary, the Stribeck curve measured at 0.5 N with the larger particles does hardly display these features. Since there is only one Stribeck curve measured at 0.5 N, it would be too blunt to state that these differences completely originate from the difference normal load. Moreover, in Figure 12b and c, the CoFs in the mixed regime are somewhat lower for the particle-lubricated systems than for the pure glycerol/water mixtures, whereas this is not observed in Figure 12a. All in all, it is difficult to find consistency in these results and give a physical explanation for them.

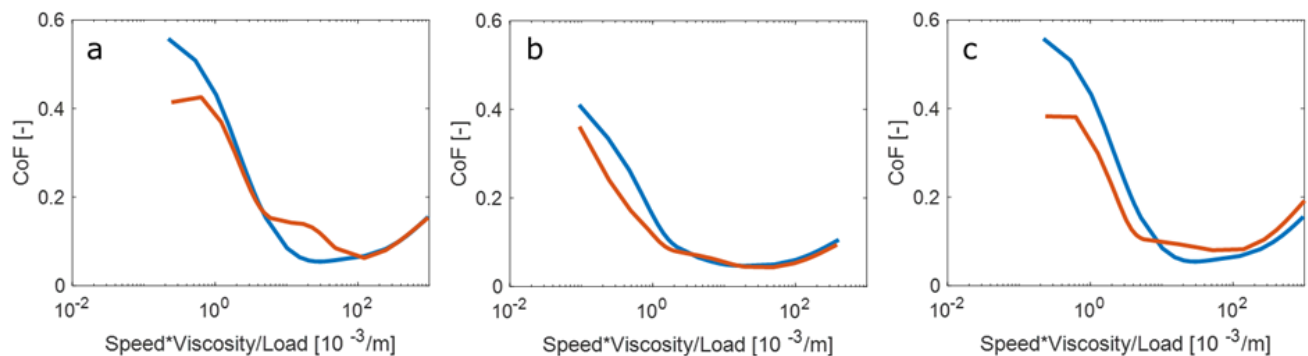


Figure 12. Stribeck curves of glycerol/water mixtures with (—) and without (—) glass microspheres measured between PDMS-rubber surfaces. (a) is at 0.2 N normal load with 45-53 μm particles, (b) at 0.5 N normal load with 45-53 μm particles and (c) at 0.2 N normal load with 20-30 μm particles. The spline fits were constructed based on measurements of gw5050, gw8020 and glycerol with and without particles.

Furthermore, it is important to note that during the experiments, it was observed that the particles were mostly pushed aside by the probe. Only by turbulence in the fluid induced by the reversal of the direction of the rec drive, particles could (temporarily) come in the path of the movement again. This suggests that the deviations of the particle mixture-lubricated curves from the pure glycerol/water curves could well be caused by single particles that (temporarily) get trapped between the probe and the substrate. This makes it even harder to give a

straightforward explanation of the results. It is yet unsure whether the features observed in the curves have a decent consistent physical basis, or are mere artifacts.

In research by Liu et al,³⁰ it was found that addition of microparticulated whey protein (MWP) particles to a water phase as lubricant leads to a considerable decrease in CoF with increasing particle concentrations up to 8% particles. This was ascribed to the ball-bearing mechanism: spherical particles can reduce the friction by effectively lowering the contact area and by changing the local relative motion from sliding to rolling. Their experiments and the experiments reported here operated at similar sliding speeds to give lubrication in the mixed regime. Still, the addition of microspheres to glycerol/water did not give an analogous decrease in CoF. One important difference between both measurement series is that Liu used a flat-bottomed PDMS probe ($d = 6 \text{ mm}$) with a glass substrate, while herein a round-bottomed PDMS probe was used on a rubber substrate. In addition, the particles in Liu's experiments were ca. $0.4 - 7 \text{ }\mu\text{m}$ in diameter, in contrast to the $20\text{-}50 \text{ }\mu\text{m}$ in diameter particles used herein. This made that in Liu's work, the particles were entrained in the contact region, as opposed to the larger particles here that were pushed out of the contact. The current geometry of the TriboLab might be not so suitable for measurements with lubricants containing the here reported particle sizes.

3.2.5 Substrate roughness

The effect of substrate roughness on the friction in a tribological measurement was investigated by performing experiments with glycerol/water mixtures between a PDMS probe as upper surface and a rough substrate as bottom surface. Substrates of different roughness were obtained by molding rubber putty on sandpaper with grit sizes P80, P120, P180 and P400 and on a petri-dish. Images of the substrates are shown in Figure A 20 in Appendix H.

Figure 13a presents the Stribeck curves obtained for glycerol/water mixtures on all different rough substrates. The primary result is that measurements on the rough substrates all give quite similar CoFs which are nearly constant over the whole range of speeds and viscosities, in contrast to the measurements on a smooth substrate. This even holds for the least rough substrate (P400), which at the first sight is more alike the smooth substrate than the roughest (Figure A 20). At low speeds and viscosities, the CoF on the rough substrates is much lower than on the smooth substrate. This might find its origin in an effectively lowered contact area for the rough substrates. Then, the probe could almost hover over the (coarse) roughness of the substrates. At higher speeds and viscosities, the lubrication on the smooth substrate approaches the hydrodynamic regime, giving low CoFs. The friction on the rough substrates shows hardly any dependence on the speed and viscosity. An explanation for this can be that the scale of the roughness is larger than the scale at which the fluid film thickness increases with higher speed and viscosity. Consequently, the lubricant has negligible influence on the contact between the surfaces; fluid entrainment never makes the fluid film much thicker than the amplitude of the roughness. This is possibly supported by the fact that for roughness P80, the friction in an unlubricated contact (Figure 13b) is similar to the friction in a lubricated contact, although 'unlubricated' should be verified for this home-made silicone rubber.

Interestingly, for a P400 substrate, the friction in the unlubricated contact is much higher than for the lubricated contact. CoFs as high as with the smooth substrate are achieved, albeit at a different speed. This could suggest that the effective contact area between the probe and the P400 substrate is increased in the unlubricated contact compared to the lubricated contact. It is supposed that pockets of liquid trapped between surfaces of low roughness may be able to form an incompressible barrier against flattening of the surfaces.³⁹ Possibly, this is what happens in the lubricated P400 contact, thereby preventing the probe from coming as close in contact with the substrate as in the unlubricated situation. For the P80 substrate, even the highest possible normal load that UMT TriboLab could apply (4 N) was not sufficient to compress the surfaces such an amount that the contact area and thus friction would increase considerably (Figure 13b). In fact, the effect of increasing the normal load is striking for neither P400 nor P80

(Figure 13b, lighter colored curves). The CoFs at 4 N normal load are lower than for 0.5 N normal load, as a result of the division by the normal load in the calculation of the CoF, see section 3.2.3. The dependence on the normal load for the P80 substrate with a lubricated contact is of the same order as for the unlubricated contact (refer to Figure A 21).

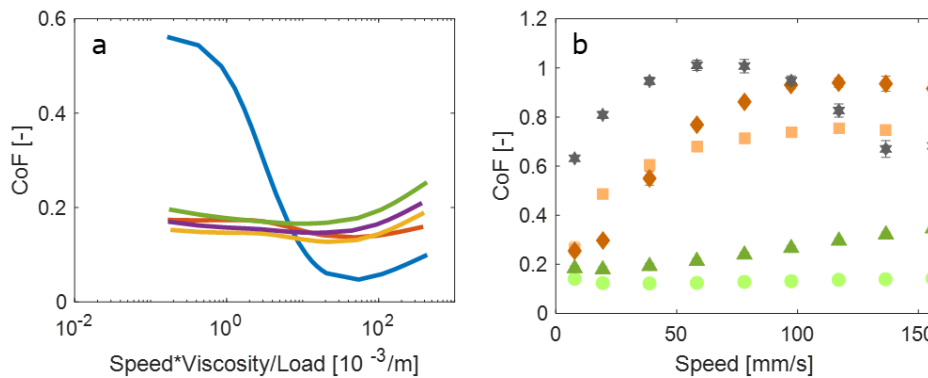


Figure 13. Tribology on rough substrates. (a) Stribeck curves of glycerol/water mixtures measured at 0.5 N between PDMS probes and substrates of roughness P80 (—), P120 (—), P180 (—), and P400 (—) and a smooth substrate (—). (b) CoF versus speed for measurements without lubricant using a PDMS probe on substrate P80 at 0.5 N (\blacktriangle) and 4 N (\bullet), substrate P400 at 0.5 N (\blacklozenge) and 4 N (\blacksquare) and on a smooth substrate at 0.5 N (\star). The curves in (a) are constructed using data of measurements with gw6040, gw8020 and glycerol. All curves in (b) use data from one measurement. Error bars indicate standard deviation.

As a final note, considering the curves of P80, P120 and P180 in Figure 13a, it seems that a higher roughness gives a slightly higher CoF. However, the fact that the curve of P400 runs across all these three curves speaks against this, although this might also be due to the seemingly different kind of surface structuring of the P400 substrate (see Figure A 20). The minimal difference in friction between the degrees of roughness might also indicate that the range of roughnesses and their amplitude and / or frequency is not in the relevant scale of roughness for tribological measurements with UMT TriboLab. Besides, in view of oral tribology, the type of roughness produced here might be not so suitable to mimic a tongue's roughness. Namely, the roughness on a tongue exists of numerous papillae (hemispherical protrusions),³¹ while the here produced roughness is based on the presence of dimples in a surfaces as a result of the molding on sandpaper.

3.3 VISCOSITY OF MILK AND SALIVA MIXTURES

The viscosity of milk, milk-salivam and milk-salt solution mixtures is presented in Figure 14. Since these fluids behave Newtonian,^{40,41} the viscosities could be measured with a rolling-ball viscometer yielding a single viscosity value for each sample. The increase in viscosity with higher whole milk content can be ascribed to the presence of fat droplets in whole milk. Addition of salivam to the mixtures gives a higher viscosity due to the high molecular weight mucin polymers. The viscosities of milk and saliva mixtures including lysozyme and tannin are very close to the values shown in Figure 14 and they are listed in Table A 1 in Appendix I. There, also the viscosities of saliva mixtures without milk are reported.

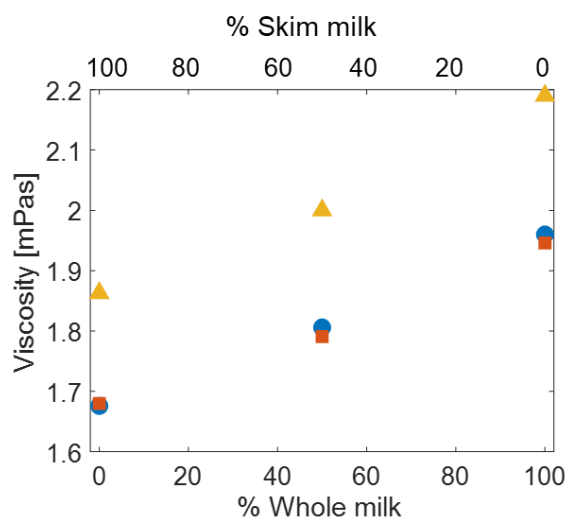


Figure 14. Viscosities of whole milk/skim milk (●) with 5% salivam (▲) and with 5% standard salt solution for saliva (■). Standard deviation falls within the marker size.

3.4 TRIBOLOGY OF MILK, SALIVA AND ASTRINGENT MIXTURES

3.4.1 Milk mixtures

Tribological experiments with whole milk and skim milk, with saliva added to milk and with the astringents lysozyme and tannic acid added to milk-saliva mixtures were performed in order to find out to which extent the UMT TriboLab could distinguish these mixtures using PDMS-rubber and steel-glass tribopairs at a standard normal load of 0.5 N. Figure 15 presents resulting Stribeck curves measured with PDMS-rubber. The sample nomenclature that is used in this chapter is explained in section 2.2. In Figure 15a, mfat100, mfat0 and mfat50 are compared with water. There is hardly a difference in CoF between the milk samples, although mfat100 gives slightly higher CoFs than mfat0 (this also holds when salt solution or salivam are added, Figure A 22d, e in Appendix J). However, for pure milk and milk-salivam, mfat50 is closer to mfat100, while for milk-salt solution it overlaps with mfat0. Moreover, with steel-glass tribopairs (Figure A 22a-c) mfat50 sometimes lies even higher than both mfat0 and mfat100. It is difficult to find a physical basis for this. Since the UMT TriboLab always gives some variation among different measurements of the same sample, it is questioned whether the differences between mfat0, mfat50 and mfat100 observed here are sufficiently significant to draw conclusions from.

Besides, the expected change in friction with fat% in the milk would be that a higher fat% gives a lower friction. This is ascribed to the coalescence and spread of fat droplets in whole milk during shearing, which is also responsible for the more creamy mouthfeel of whole milk.¹⁶ It was indeed found by Chojnicka-Paszun et al.¹⁴ that the friction coefficient decreased

significantly as a function of fat% in milk (from a threshold of 1% fat). In that work, a mini traction machine (MTM) with rubber surfaces operated at 5 N normal load was used as tribological setup. Perhaps, the current experimental setup of the TriboLab does not induce coalescence of fat droplets, and thus does not give substantial differences in friction for milk with varying fat%. Findings of Dresselhuis et al.³⁴ would underpin this: they found that depending on the tribopairs, coalescence of emulsions droplets might or might not occur. Using a pig's tongue probe on a glass surface induced droplet coalescence, while using a PDMS probe did not. Moreover, the crucial dependence of the friction response on the used system was also denoted by Laguna et al,⁴² who were not able to measure differences in CoF between skim milk and whole milk with a MTM with PDMS surfaces, whereas for yoghurt and cream cheese, the fat content had a significant influence on the friction.

Remarkably, there is a clear difference between the CoFs of the milks and water in Figure 15a. This suggests that the friction measured mainly originates from the proteins present in milk, possibly by adsorption on the surfaces.

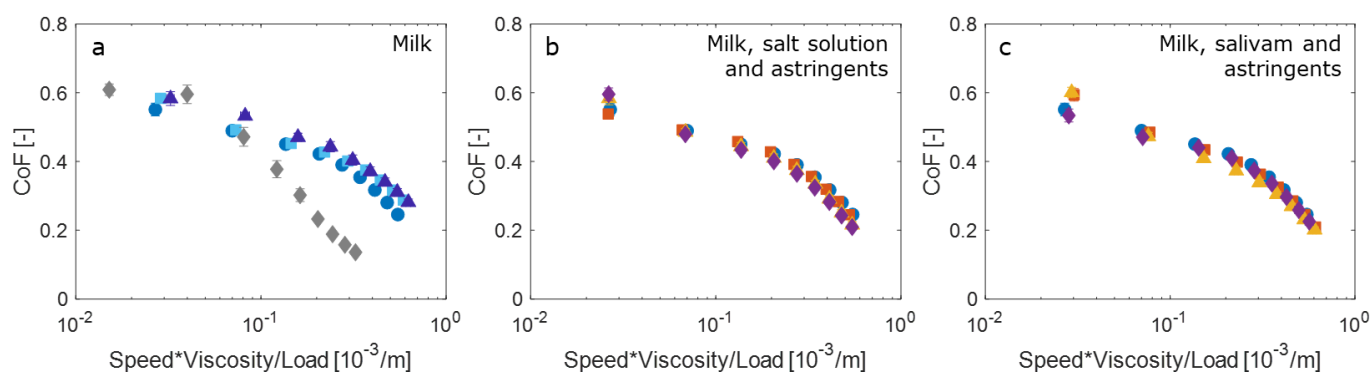


Figure 15. Stribeck curves of milk, saliva and astringent mixtures measured at 0.5 N with PDMS-rubber tribopairs. (a) Mfat0 (●), mfat50, (■), mfat100 (▲) and water (◆). (b) Mfat0 (●), mfat0-s (■), mfat0-s-lys (▲), mfat0-s-tan (◆). (c) Mfat0 (●), mfat0-sm (■), mfat0-sm-lys (▲), mfat0-sm-tan (◆).

Figure 15b and c show friction curves of mfat0 with salt solution or salivam and with tannic acid or lysozyme added to these mixtures. No influence of the addition of any of these substances to milk can be observed, despite the possible complexation of astringents with proteins (in saliva and / or milk), which could have led to a loss in lubrication. The same holds for the experiments with steel-glass tribopairs (Figure A 22f, g), although there it seems that mfat0 gives a lower friction than the rest of the solutions. It is possible that the concentration in which the saliva and astringents were added to the milk was so low that the properties of milk outweigh the potential influence of these substances on the friction. However, in the experiments of Laguna et al,⁴² no significant effect of saliva addition to milk was observed even though their mixing ratio product: saliva was 1:1. Again, the system and surfaces used are likely to contribute strongly to which distinctions in friction between samples can be measured. Besides, it might be more physiologically relevant to absorb a salivary film onto the tribopairs instead of pre-mixing the sample with saliva.⁴³ In addition, concerning the effect of astringents, the concentration of astringents used here is of the same order or even higher than the average phenolics content in tea or tannins content in wine,^{44,45} so it would be useful if the tribometer could measure an effect on the friction when astringent substances are present in such concentrations.

3.4.2 Saliva and astringents

In addition to the milk mixtures with saliva and astringents, experiments with the pure solutions of tannic acid and lysozyme in salivam and salt solution were carried out to probe the effect of the addition of astringents on the friction. The lubricating ability of salivam should result from the mucin polymers, and therefore measurements with saliva without mucin (the salt solution) were carried out as a blank. On the basis of sensory evaluation of the effect of adding tannin

and lysozyme to drinks,^{22,46} it is expected that the addition of these astringent substances to saliva would lead to an increase in friction coefficient, as a result of the loss of lubricating ability of the saliva engendered by complexation of astringents with salivary proteins (the mucins here).¹³ This is, however, not what is directly observed from the Stribeck curves of salivam, sm-lys and sm-tan shown in Figure 16a and c. Using PDMS-rubber tribopairs, the friction of salivam lies in between sm-tan and sm-lys. It was observed that tannic acid formed large aggregates when added to salivam (compare Figure 17a and c). Precipitation of these aggregates might indeed have led to a slight increase in CoFs of sm-tan compared to salivam. The microscopic structure of sm-lys (Figure 17b) is fairly different from that of sm-tan. The dense protein network (consisting of relatively small aggregates) might, under influence of turbulence, not precipitate but form an extra hydrating layer on the surfaces, whereby it acts as extra salivary protein, decreasing the friction.

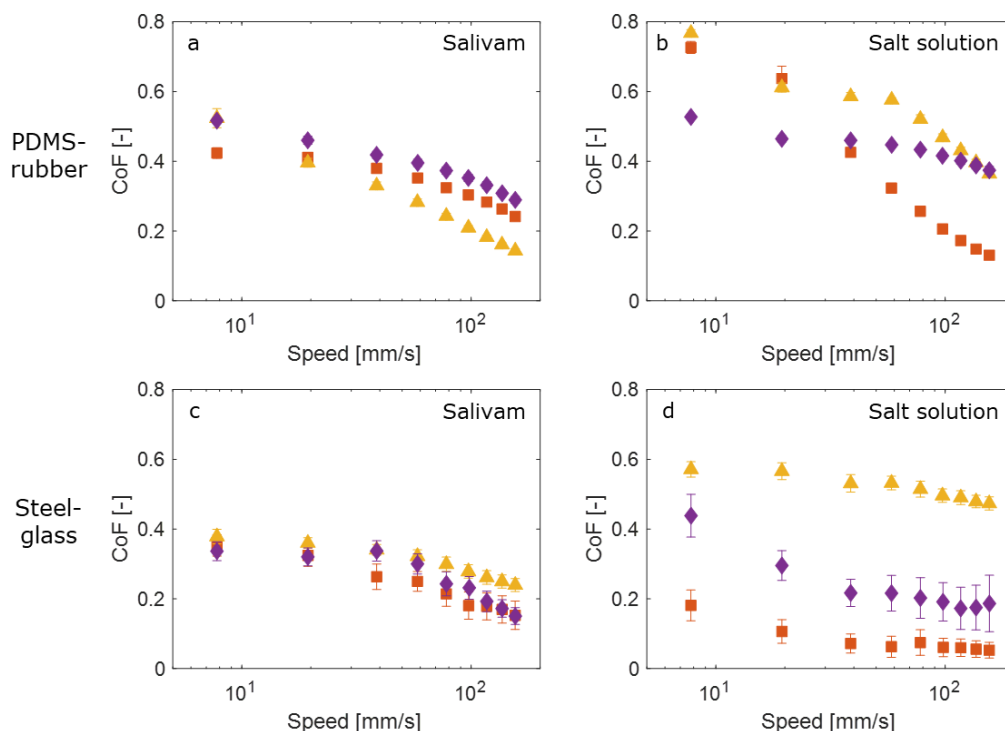


Figure 16. Stribeck curves of saliva and astringent mixtures measured at a load of 0.5 N with PDMS-rubber (a-b) and steel-glass (c-d) tribopairs. (■) = pure salt solution or salivam as indicated in each figure, (▲) = with 2% lysozyme and (◆) = with 2% tannic acid. Error bars indicate standard deviation.

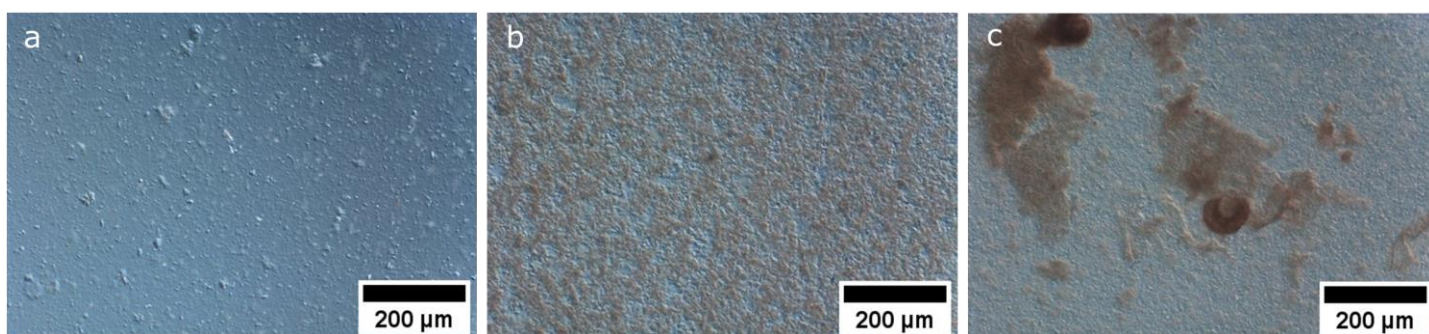


Figure 17. Microscopy images of salivam (a), sm-lys (b) and sm-tan (c).

On closer inspection of Figure 16a, it can be seen that at the lowest speeds (7-15 mm/s) both sm-lys and sm-tan have a higher CoF than salivam. In the case of sm-lys, the low sliding speed might have allowed the tribometer to detect an effect of some depletion of aggregates. This could suggest that only at the lowest speeds the lubrication is representative for the in-mouth

conditions at which astringency is perceived, albeit that the mechanisms behind oral perception of astringency are probably more complicated than purely protein precipitation.²¹ Still, it might be true that oral tribology is best mimicked at the lowest sliding speeds, considering the CoFs of salivam and salt solution at low speeds (clearly represented in Figure A 23a in Appendix K). Only at speeds below ca. 30 mm/s, salivam has better lubricating properties than the salt solution in this tribological system comprising PDMS-rubber tribopairs operated at 0.5 N normal load. It is indeed true that in oral conditions, the typical speed of tongue movement is low (2-30 mm/s).⁴⁷ The fact that with the steel-glass tribopair the CoFs for salivam are always higher than for the salt solution (Figure A 23b) raises the question whether steel-glass is an appropriate system for oral tribology. Actually, at present, PDMS tribopairs are generally considered the most feasible for oral tribology.¹⁸ The differences in friction between salivam, sm-lys and sm-tan with steel-glass (Figure 16c) are also very different from these with PDMS-rubber, maybe due to different interactions of the surfaces with the proteins / molecules in the solutions or due to the difference in contact geometry (two stiff and smooth materials will give another gap size and contact area than two softer materials).

Despite having given some suggestions concerning the differences between salivam, sm-lys and sm-tan, the significance and physical origin of these still remain unsure. Be that as it may, the effect that tannic acid and lysozyme have on the friction of the salt solutions is certainly significant (Figure 16b, d). Compared to that, the effect of these substances on salivam is little. It seems that mucin plays a crucial role in mitigating the changes in friction when an astringent substance is added. Perhaps, interactions of the s-lys and s-tan solution with the substrate lead to a substantial change in friction compared to the salt solution, while for salivam the influence of tannic acid or lysozyme in itself is weakened due to the formation of aggregates. Note also that with PDMS-rubber tribopairs, the lubrication of salivam seems to be more in the boundary regime than the lubrication with salt solution (which spans the whole mixed regime), even though salivam has a higher viscosity than the salt solution. The comparison of these Stribeck curves is more clearly shown in Figure A 23c. This suggests that mucin plays a surface active role, rendering the tribopair surfaces effectively more in contact than without mucin. The tribopair materials have a large impact on the shape and the mutual order of the Stribeck curves of the salt solution, s-lys and s-tan. This points to the importance of the tribopairs's physical and / or chemical material properties in determining the friction.

On the whole, the tribology of saliva with tannic acid or lysozyme with the UMT TriboLab is not trivial and it is difficult to make a straightforward connection to oral tribology. At the same time, the experiments give some useful information about what differences in product properties can be measured with the UMT TriboLab with the current measurement protocols. The effect of the tribopair choice on the resulting friction curves is large.

4 CONCLUSIONS

The effect of several sample, material and operation parameters on the friction measured with Bruker's UMT TriboLab was investigated.

- As predicted by the Stribeck curve model, an increase in glycerol/water sample viscosity and entrainment speed shifts the lubrication from the boundary towards the hydrodynamic regime. A master Stribeck curve can be obtained by scaling the speed with the viscosity.
- Stribeck curves obtained with particles of 20-50 μm added to glycerol/water mixtures are difficult to interpret. It is likely that the current geometry of the TriboLab (a point contact between a round-bottomed PDMS probe and a rubber substrate) is not so appropriate for such systems.
- Using rough substrates produced by molding and curing rubber putty on sandpaper yields Stribeck curves where the friction coefficient is low compared to the friction coefficient in the boundary and mixed regime on a smooth substrate, and is hardly dependent on the speed and sample viscosity. Probably, the (coarse) roughness results in an effectively lowered contact area between probe and substrate, giving low friction and little influence of the lubricant.
- Increasing the normal load force during tribological measurements with glycerol/water mixtures decreases the friction coefficients in the mixed (and boundary) regime. Apparently, the friction force is less than linearly dependent on the load force.
- PDMS-rubber tribopairs show traces of wear after the measurements. The size of the wear spot on the PDMS probe is indicative of the contact area between probe and substrate, and increased linearly with normal load.
- The use of steel-glass, PDMS-glass and steel-rubber tribopairs in addition to the standard PDMS-rubber tribopairs shows that friction coefficients in the mixed regime decrease with an increase in smoothness and stiffness of the tribopair materials. PDMS-rubber gives a more extended mixed regime than steel-glass.
- Comparison of measurements with sunflower oil and glycerol/water on PDMS-rubber and steel-glass demonstrates that the wettability of the tribopairs affects the lubricity (in the mixed regime). The fluid that wets the substrate better is the better lubricant.
- In the hydrodynamic regime of the Stribeck curves of glycerol/water mixtures, the influence of both the normal load and the tribopair materials diminishes, giving overlapping Stribeck curves at the different conditions. This confirms that fluid properties here prevail over asperity contacting.
- The crucial dependence of the friction coefficient on the tribopair materials is also manifest in the tribological experiments with milk, saliva and astringent mixtures. In general, steel-glass tribopairs give less dependence of the friction coefficient on the speed and sample viscosity than PDMS-rubber. For the saliva and astringent mixtures, the mutual order of the Stribeck curves even changes when using other tribopair materials.
- With the current tribometer setup, it was not possible to significantly distinguish milks with different fat content. The addition of saliva did not influence the friction too.
- The addition of tannic acid and lysozyme (representative astringent substances) to saliva has a non-trivial effect on the friction. The friction coefficients of saliva-astringent mixtures and salt solution being higher than the friction coefficient of purely saliva at the lowest entrainment speeds with PDMS-rubber tribopairs, might indicate that these conditions give the best system for oral tribology with UMT TriboLab to date.

5 OUTLOOK

It was noted that in some instances there was a considerable spread in the CoFs across different measurements of the same sample using the same protocol (as shown in Figure A 16). The use of each time a different PDMS probe and different (position on a) rubber substrate, might play an important role in this. Consequently, it can sometimes not be determined unambiguously whether small differences in CoF between different samples (e.g. the milks in Figure 15 and Figure A 22) are significant. Therefore, it could be practical to perform a kind of method validation for the UMT TriboLab, in the first place by systematically examining the spread that the UMT TriboLab gives in the data of multiple measurements of the same sample. One could for example measure a sample eight times on the same substrate (at a different position, and always using a different PDMS probe) and also eight times on a different substrate and calculate the standard deviations. This would provide an impression of the precision of the measurements. This could then be done for each type of product that is measured on the TriboLab.

If one might want to characterize samples or products with colloidal particles, it could be better to use a probe that has a flatter bottom than the current PDMS probes. This could overcome the problem of particles being pushed out of the track. However, it might be difficult to maintain a constant pressure in the whole contact area in such a system.

With the current PDMS-rubber and steel-glass tribopairs, it was not possible to find a significant difference in the friction coefficients of milks with different fat content. Other research provides strong evidence that it should be possible to distinguish the tribological properties of skim and whole milk.¹⁴ A possible option to achieve that with the UMT TriboLab would be to use other tribopairs, e.g. somewhat rougher PDMS probes, since the material type may affect whether or not emulsion droplets (fat droplets in milk) coalesce and form a lubricating layer.³⁴ To mimic the roughness of the tongue best, the roughness should be based on asperities and not on dimples.

The tribological experiments with saliva and astringents seem to indicate that the measurements at the lowest speed with PDMS-rubber tribopairs are the most representative for the in-mouth lubrication. Therefore, it could be useful to focus on lubrication at low entrainment speeds in a soft contact such as PDMS-rubber, and investigate with other (astringent) food systems whether the tribological properties under these conditions can be related to the sensory perception.

As follow-up to the experiments with tannic acid and lysozyme, tribological experiments with real food systems which provoke a sensation of astringency, such as (instant) the or red wine, could be carried out. In principle, these systems should cause an increase in friction due to reduced salivary lubricity.

ACKNOWLEDGEMENTS

I want to thank M. Adamse and S. de Jong for making me familiar with equipment on the laboratory.

I am very grateful to Edwin Lijffijt for conducting a part of the tribological experiments for me while I was forced to stay at home because of the corona situation.

I would like to thank R. H. Tromp for his supervision during my project and I want to thank E. de Hoog for the discussion of and feedback on my results.

Finally, I would like to thank NIZO for giving me the opportunity to carry out my internship there.

REFERENCES

1. Shaffer, S. J. Tribology 101 – Introduction to the Basics of Tribology. *Bruker* (2013).
2. Torbacke, M., Rudolphi, A. K. & Kassfeldt, E. *Lubricants - Introduction To Properties and Performance*. (John Wiley & Sons Ltd, 2014).
3. Tichy, J. A. & Meyer, D. M. Review of solid mechanics in tribology. *Int. J. Solids Struct.* **37**, 391–400 (2000).
4. Prakash, S., Tan, D. D. Y. & Chen, J. Applications of tribology in studying food oral processing and texture perception. *Food Res. Int.* **54**, 1627–1635 (2013).
5. Hersey, M. D. The laws of lubrication of horizontal journal bearings. *J. Washingt. Acad. Sci.* **4**, 542–552 (1914).
6. De Vicente, J., Stokes, J. R. & Spikes, H. A. Lubrication properties of non-adsorbing polymer solutions in soft elastohydrodynamic (EHD) contacts. *Tribol. Int.* **38**, 515–526 (2005).
7. de Vicente, J., Stokes, J. R. & Spikes, H. A. Soft lubrication of model hydrocolloids. *Food Hydrocoll.* **20**, 483–491 (2006).
8. Sudhakar, A., Jithender, B. & Mishra, A. Importance of tribology in food and dairy industries: An overview. *J. Pharmacogn. Phytochem.* **9**, 418–422 (2020).
9. Chen, J. & Stokes, J. R. Rheology and tribology: Two distinctive regimes of food texture sensation. *Trends Food Sci. Technol.* **25**, 4–12 (2012).
10. Prakash, S. From Rheology to Tribology: Applications of Tribology in Studying Food Oral Processing and Texture Perception. in *Advances in Food Rheology and Its Applications* 65–86 (Elsevier Ltd, 2017). doi:10.1016/B978-0-08-100431-9.00004-8
11. PCS Instruments. How are you quantifying sensory perception? (2018). Available at: <https://pcs-instruments.com/articles/how-are-you-quantifying-sensory-perception/>. (Accessed: 14th March 2020)
12. Kokini, J. L. The physical basis of liquid food texture and texture-taste interactions. *J. Food Eng.* **6**, 51–81 (1987).
13. de Wijk, R. A. & Prinz, J. F. The role of friction in perceived oral texture. *Food Qual. Prefer.* **16**, 121–129 (2005).
14. Chojnicka-Paszun, A., de Jongh, H. H. J. & de Kruif, C. G. Sensory perception and lubrication properties of milk: Influence of fat content. *Int. Dairy J.* **26**, 15–22 (2012).
15. Euston, S. R. Emulsifiers in Dairy Products and Dairy Substitutes. in *Food Emulsifiers and Their Applications* (eds. Hasenhuettl, G. L. & Hartel, R. W.) (Springer Science+Business Media, LLC, 2008). doi:10.1007/978-0-387-75284-6
16. Dresselhuis, D. M., de Hoog, E. H. A., Cohen Stuart, M. A., Vingerhoeds, M. H. & van Aken, G. A. The occurrence of in-mouth coalescence of emulsion droplets in relation to perception of fat. *Food Hydrocoll.* **22**, 1170–1183 (2008).
17. Upadhyay, R., Brossard, N. & Chen, J. Mechanisms underlying astringency: introduction to an oral tribology approach. *J. Phys. D. Appl. Phys.* **49**, 104003 (2016).
18. Sarkar, A., Andablo-Reyes, E., Bryant, M., Dowson, D. & Neville, A. Lubrication of soft oral surfaces. *Curr. Opin. Colloid Interface Sci.* **39**, 61–75 (2019).
19. van Nieuw Amerongen, A., Bolscher, J. G. M. & Veerman, E. C. I. Salivary proteins: Protective and diagnostic value in cariology? *Caries Res.* **38**, 247–253 (2004).
20. Gibbins, H. L. & Carpenter, G. H. Alternative Mechanisms of Astringency - What is the Role of Saliva? *J. Texture Stud.* **44**, 364–375 (2013).
21. Rossetti, D., Bongaerts, J. H. H., Wantling, E., Stokes, J. R. & Williamson, A.-M. Astringency of tea catechins: More than an oral lubrication tactile percept. *Food Hydrocoll.* **23**, 1984–1992 (2009).
22. Brossard, N., Cai, H., Osorio, F., Bordeu, E. & Chen, J. "Oral" Tribological Study on the Astringency Sensation of Red Wines. *J. Texture Stud.* **47**, 392–402 (2016).
23. Delius, J., Médard, G., Kuster, B. & Hofmann, T. Effect of Astringent Stimuli on Salivary Protein Interactions Elucidated by Complementary Proteomics Approaches. *J. Agric. Food Chem.* **65**, 2147–2154 (2017).
24. Upadhyay, R. & Chen, J. Smoothness as a tactile percept: Correlating 'oral' tribology with sensory measurements. *Food Hydrocoll.* **87**, 38–47 (2019).
25. Imai, E., Hatae, K. & Shimada, A. Oral perception of grittiness: effect of particle size and concentration of the dispersed particles and the dispersion medium. *J. Texture Stud.* **26**, 561–576

- (1995).
26. Cayot, P., Schenker, F., Houzé, G., Sulmont-Rossé, C. & Colas, B. Creaminess in relation to consistency and particle size in stirred fat-free yogurt. *Int. Dairy J.* **18**, 303–311 (2008).
 27. Laiho, S., Williams, R. P. W., Poelman, A., Appelqvist, I. & Logan, A. Effect of whey protein phase volume on the tribology, rheology and sensory properties of fat-free stirred yoghurts. *Food Hydrocoll.* **67**, 166–177 (2017).
 28. Liu, K., Stieger, M., van der Linden, E. & van de Velde, F. Tribological properties of rice starch in liquid and semi-solid food model systems. *Food Hydrocoll.* **58**, 184–193 (2016).
 29. Wu, Y. Y., Tsui, W. C. & Liu, T. C. Experimental analysis of tribological properties of lubricating oils with nanoparticle additives. *Wear* **262**, 819–825 (2007).
 30. Liu, K., Tian, Y., Stieger, M., Van der Linden, E. & Van de Velde, F. Evidence for ball-bearing mechanism of microparticulated whey protein as fat replacer in liquid and semi-solid multi-component model foods. *Food Hydrocoll.* **52**, 403–414 (2016).
 31. Ranc, H., Servais, C., Chauvy, P.-F., Debaud, S. & Mischler, S. Effect of surface structure on frictional behaviour of a tongue/palate tribological system. *Tribol. Int.* **39**, 1518–1526 (2006).
 32. Krzeminski, A., Wohlhüter, S., Heyer, P., Utz, J. & Hinrichs, J. Measurement of lubricating properties in a tribosystem with different surface roughness. *Int. Dairy J.* **26**, 23–30 (2012).
 33. Di Cicco, F., Oosterlinck, F., Tromp, H. & Sein, A. Comparative study of whey protein isolate gel and polydimethylsiloxane as tribological surfaces to differentiate friction properties of commercial yogurts. *Food Hydrocoll.* **97**, 105204 (2019).
 34. Dresselhuis, D. M., de Hoog, E. H. A., Cohen Stuart, M. A. & van Aken, G. A. Application of oral tissue in tribological measurements in an emulsion perception context. *Food Hydrocoll.* **22**, 323–335 (2008).
 35. Stee, M. van, Hoog, E. de & Velde, F. van de. Oral Parameters Affecting Ex-vivo Tribology. *Biotribology* **11**, 84–91 (2017).
 36. Witten, T. A. Structured Fluids. *Phys. Today* **43**, 21–28 (1990).
 37. Goodwin, J. W. & Hughes, R. W. Chapter 1 - Introduction. in *Rheology for Chemists: An Introduction* (Royal Society of Chemistry, 2008).
 38. Engineering ToolBox. Young's Modulus - Tensile and Yield Strength for common Materials. (2003). Available at: https://www.engineeringtoolbox.com/young-modulus-d_417.html. (Accessed: 22nd June 2020)
 39. Bongaerts, J. H. H., Fourtouni, K. & Stokes, J. R. Soft-tribology: Lubrication in a compliant PDMS–PDMS contact. *Tribol. Int.* **40**, 1531–1542 (2007).
 40. Morison, K. R., Phelan, J. P. & Bloore, C. G. Viscosity and non-newtonian behaviour of concentrated milk and cream. *Int. J. Food Prop.* **16**, 882–894 (2013).
 41. Hatton, M. N., Levine, M. J., Margarone, J. E. & Aguirre, A. Lubrication and Viscosity Features of Human Saliva and Commercially Available Saliva Substitutes. *J. Oral Maxillofac. Surg.* **45**, 496–499 (1987).
 42. Laguna, L., Farrell, G., Bryant, M., Morina, A. & Sarkar, A. Relating rheology and tribology of commercial dairy colloids to sensory perception. *Food Funct.* **8**, 563–573 (2016).
 43. Pradal, C. & Stokes, J. R. Oral tribology: bridging the gap between physical measurements and sensory experience. *Curr. Opin. Food Sci.* **9**, 34–41 (2016).
 44. Aleixandre-Tudo, J. L., Nieuwoudt, H., Aleixandre, J. L. & Du Toit, W. J. Robust Ultraviolet–Visible (UV–Vis) Partial Least-Squares (PLS) Models for Tannin Quantification in Red Wine. *J. Agric. Food Chem.* **63**, 1088–1098 (2015).
 45. Kodama, D. H., Goncalves, A. E. S. S., Lajolo, F. M. & Genovese, M. I. Flavonoids, total phenolics and antioxidant capacity: comparison between commercial green tea preparations. *Cienc. e Tecnol. Aliment.* **30**, 1077–1082 (2009).
 46. Vingerhoeds, M. H., Silletti, E., de Groot, J., Schipper, R. G. & van Aken, G. A. Relating the effect of saliva-induced emulsion flocculation on rheological properties and retention on the tongue surface with sensory perception. *Food Hydrocoll.* **23**, 773–785 (2009).
 47. Hiemae, K. M. & Palmer, J. B. Tongue Movements in Feeding and Speech. *Crit. Rev. Oral Biol. Med.* **14**, 413–429 (2003).
 48. Wikipedia contributors. Sandpaper. *Wikipedia, The Free Encyclopedia* (2020). Available at: https://en.wikipedia.org/wiki/Sandpaper#Grit_sizes. (Accessed: 29th May 2020)

APPENDICES

APPENDIX A. DATA ANALYSIS

A1: Data processing

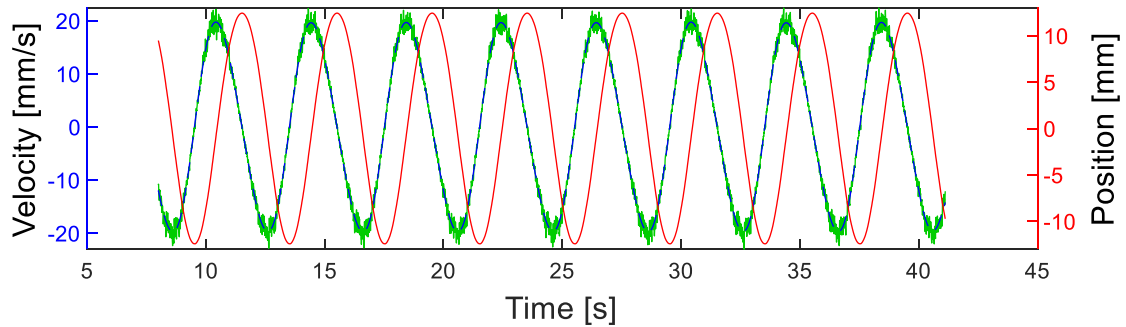


Figure A 1. Velocity and position of the rec drive versus time for a tribological measurement with sunflower oil at a rec drive frequency of 0.25 Hz. The green line is the non-smoothed velocity.

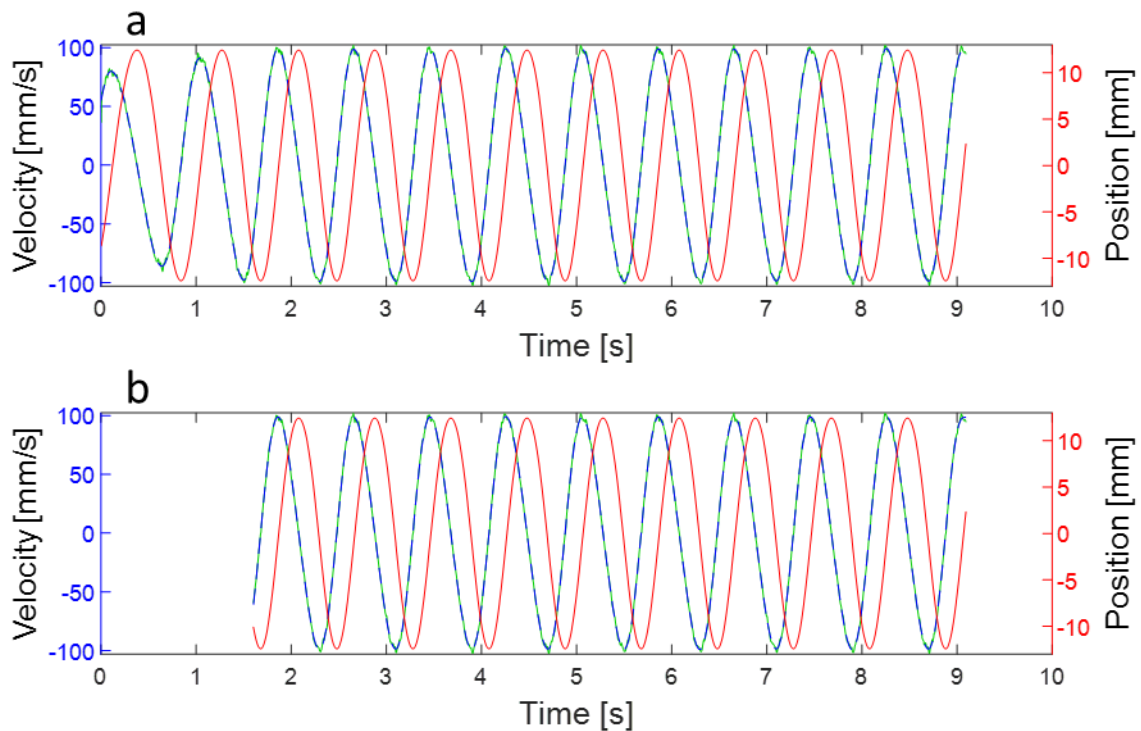


Figure A 2. Time clipping in the data of a tribological measurement with sunflower oil at a rec drive frequency of 1.25 Hz. (a) velocity and position without time clipping. (b) velocity and position after time clipping. All data in the first 2 / Hz second of each step is rejected.

A2: Comparison: CoF via Oscil.COF in UMT Viewer software vs CoF from raw data

In section 2.6 is explained how CoFs are calculated using the raw data output of the UMT TriboLab. Another way to obtain CoFs is using the UMT Viewer software. The option Oscil.COF in the Viewer software applies an oscillating test to the measurement data to compensate for the positive and negative friction force (two directions of movement). In the standard method, it uses 50% of the data points around the maximum speed. A selection of time and CoF data points (ca. ten per step) is exported. The resulting CoF per step is the mean of these ca. ten data points. To find the average speed in each step, raw data of one measurement at the step with rec drive frequency of 1 Hz was used. The speed for each data point was calculated (Δ LVDT / Δ time), and from this the average speed was calculated using 50% of the data points below the maximum speed (same criterion for data selection as for CoF calculation). This was done for one measurement, and the resulting speed value (70.29 mm/s) is used as a standard value for the up to 50% below maximum average rec drive speed at 1 Hz. Speeds in the other steps were obtained by multiplying 70.29 mm/s with the respective frequency of the step.

Figure A 3 displays the friction versus speed curves of one measurement of sunflower oil calculated via the raw data analysis and via the UMT Viewer Oscil.COF option. The shape of the curves shows a very good agreement, although the speeds obtained with the latter method lie consequently below these obtained with the former method. This is a result of the difference in data selection criterion between the two methods, where in the raw data analysis speeds down to 5% below the maximum speed are used while with the Oscil.COF option 50% of the data points below the maximum speed are used.

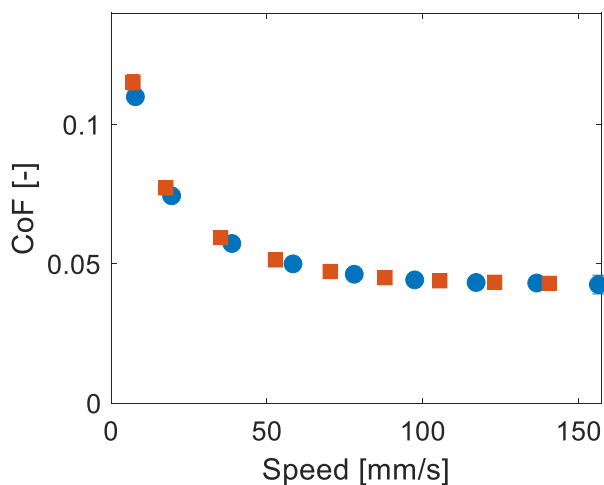


Figure A 3. Friction vs speed curve of sunflower oil measured at 0.5 N normal load with PDMS-rubber tribopairs, calculated via the raw data (●) and via the UMT Viewer Oscil.COF option (■).

APPENDIX B. STRIBECK CURVES DIFFERENT TRIBOPAIRS

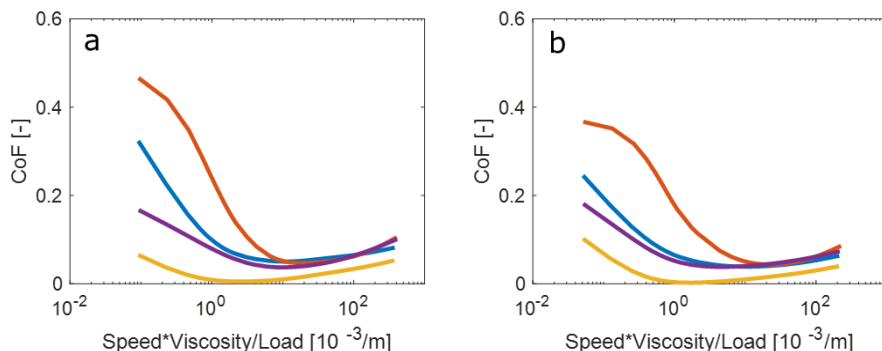


Figure A 4. Stribeck curves of glycerol/water mixtures measured at 0.5 N (a) and 0.9 N (b) normal load with PDMS-rubber (—), PDMS-glass (—), steel-rubber (—) and steel-glass (—) tribopairs. The curves are spline interpolations of separate data points.

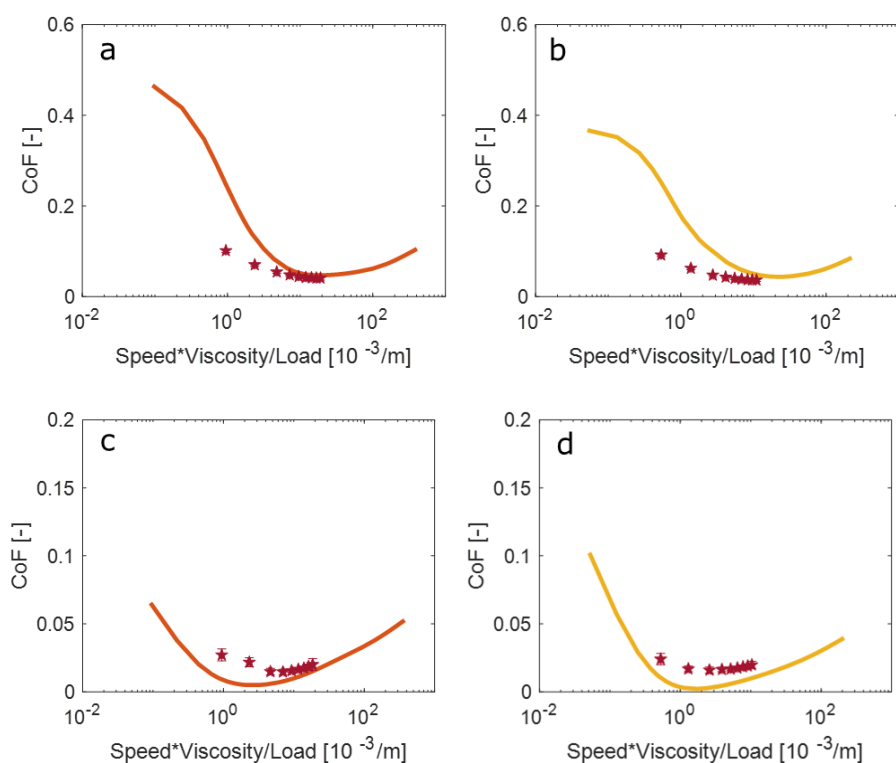


Figure A 5. Stribeck curves of glycerol/water mixtures measured at 0.5 N (—) and 0.9 N (—) and of sunflower oil (★) measured at these normal loads. Tribopairs: PDMS-rubber (a-b) and steel-glass (c-d).

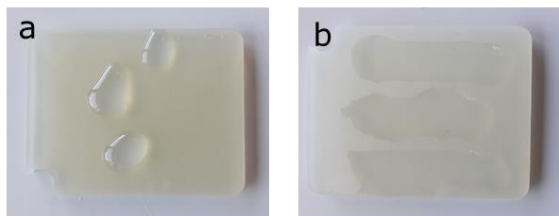


Figure A 6. Silicone rubber substrate with gw5050 (a) and sunflower oil (b). sunflower oil spreads well on the substrate, as opposed to gw5050. This indicates that the rubber is hydrophobic.

APPENDIX C. WEAR

In section 3.2.2 it was mentioned that after a measurement with PDMS-rubber tribopairs, clear signs of wear can be observed on the probe and substrate. Figure A 7 shows a typical wear spot on a PDMS probe after a tribological measurement on a rubber substrate. Figure A 8a-c show the track formation on rubber substrates after measurements at 0.2 N and 0.5 N normal load. The substrates were imaged with CLSM (d-f) as well to gain more insight in the nature of the track formation. Interestingly, the tracks are not continuous, but comprise several scratches. These scratches might originate from tiny pieces of rubber that are dragged with the PDMS probe (which is slightly rough such that pieces can attach to it). However, from the CSLM images it is not possible to tell whether the tracks have a physical depth or are an effect of structure modification and are a refractive index effect.

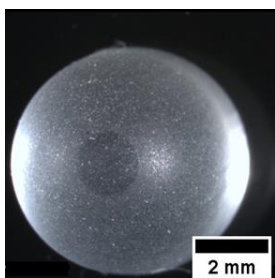


Figure A 7. Stereomicroscopy image of a PDMS probe after a tribological measurement with gw6040 on a rubber substrate at 0.5 N normal load.

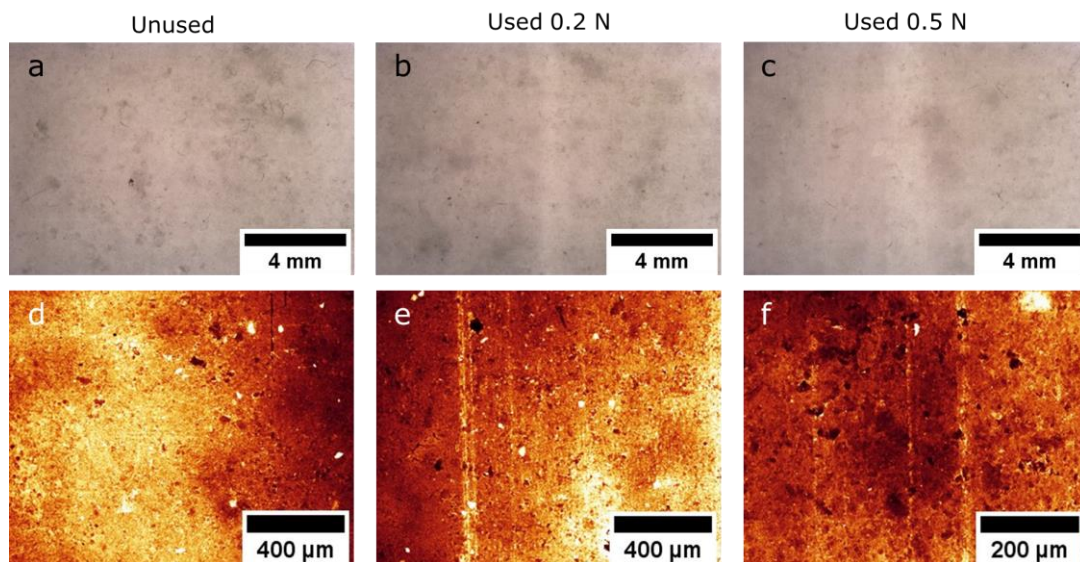


Figure A 8. Stereomicroscopy (transmissive light) (a-c) and CLSM (d-f) images of a rubber substrate before (a, d) and after (b, c, e, f) a tribological measurement with a glycerol/water mixture using PDMS-rubber tribopairs at 0.2 N and 0.5 N normal load.

The effect of wear on the measured friction is clearly noticed when comparing three sequential measurements using the same PDMS probe at the same position on the rubber substrate (so at the track where was already measured), see Figure A 9a. The CoF decreases over the three measurements. Probably, the surface of the probe and the substrate in contact gets smoother by the rubbing of the materials against each other. Curiously, the largest decrease in CoF occurs at medium speeds, while the drop in CoF at low speeds is limited. To distinguish between the wear of the probe and the wear of the substrate, measurements with the same probe but on a different track, and with a different probe on the same track were carried out. Figure A 9b, where the same probe is used, shows a similar decrease in friction over the three measurements as Figure A 9a, while Figure A 9c, where is only measured on the same track, shows a significantly lower drop in CoF. This could have been expected, since the probe is continuously rubbed over the course of a measurement, while the wear of the substrate is distributed over the whole stroke. It could also play a small role that the PDMS probe is slightly softer than the rubber substrate.

For PDMS-glass and steel-rubber tribopairs, no traces of wear could be observed on the PDMS probe and rubber substrate after a measurement. This is reflected in the very slight decrease in CoF over three measurement with steel-rubber tribopairs (Figure A 9d). Remarkably, the decrease in CoF over sequential measurements with PDMS-glass mostly depends on the renewing of the sample in between measurements, while using the same glass plate and same PDMS probe. When three sequential measurements are carried out with the same probe and with the same aliquot of sample on the glass plate, there is a slight decrease in the CoF (Figure A 9e). There is no decrease in CoF when a new aliquot of sample is put on the glass plate between the measurements (Figure A 9f). A possible origin for this is that when using the same aliquot, the sample is already spread out at the beginning of the 2nd and the 3rd measurement. But in principle, the structure and properties of glycerol/water mixtures (simple fluids) should not be altered upon shearing. The difference might also have to do with the time frame in which the measurements were repeated; the time between two measurements is longer when the sample has to be renewed in between. Perhaps, a PDMS probe undergoes relaxation during a measurement and needs some time to return to its original state. When during this 'back-relaxation' a new measurement is started, the slight difference in PDMS structure might give some deviation in CoF.

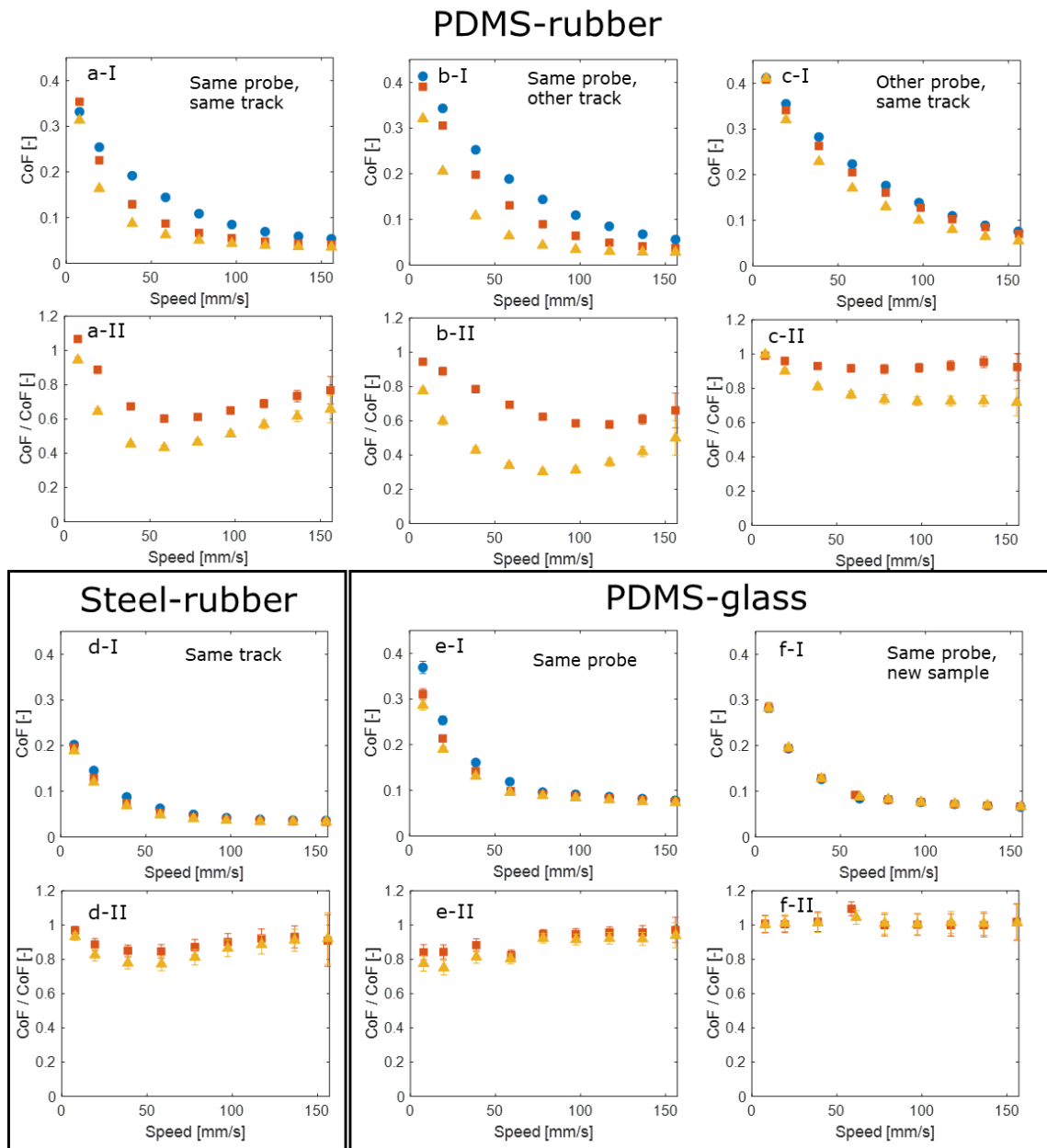


Figure A 9. CoF versus speed curves of sequential tribological measurements with gw6040 as lubricant at 0.5 N normal load using PDMS-rubber (a-c), steel-rubber (d) and PDMS-glass (e-f) tribopairs. Measurement conditions are reported in the figures. The same glass plate and steel probe are used in all measurements. Figures -I: curves of the 1st (●), 2nd (■) and 3rd (▲) consecutive measurement. Figures -II: relative change in CoF expressed in 2nd / 1st (■) and 3rd / 1st measurement (▲). The decrease in CoF over the different measurements is indicative of wear.

APPENDIX D. FRICTION FORCE

Instead of reporting the friction of a tribological measurement in terms of the CoF, also purely the friction force can be used. Then, the normal load force that the ball probe exerts on the substrate is not taken into account. For illustration, Figure A 10a presents the Stribeck curves of glycerol/water mixtures with PDMS-rubber tribopairs at normal loads 0.2 N, 0.5 N and 0.9 N using the friction force (note that the x-axis is also not scaled with the normal load). The curves at the different loads have now reversed in order (compare Figure 10a). Figure A 10b shows even more clearly the difference between the dependence of the CoF and of the friction force on the normal load. The figure gives the values of the CoF and the friction force for the sample gw5050 measured on PDMS-rubber tribopairs in the step with a rec drive speed of 0.1 Hz at the three normal loads. Here, the lubrication is in the transition from boundary to mixed regime. It is logical that with a higher normal load the friction force increases, since the asperity contact increases with higher load. Because the differences in friction force for each higher load are not as large as the differences in normal load (i.e. the friction force is less than linearly dependent on the normal load), the resulting CoFs decrease with increasing normal load.

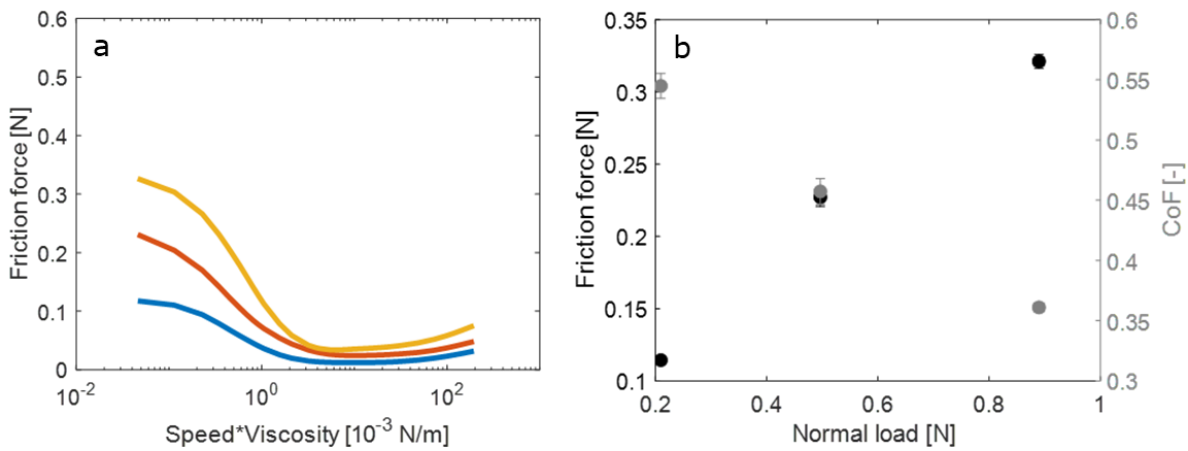


Figure A 10. (a) Stribeck curve (using friction force instead of CoF) of glycerol/water mixtures measured at 0.2 N (—), 0.5 N (—) and 0.9 N (—) normal load with PDMS-rubber tribopairs. (b) Dependence of the friction force and the CoF on the normal load for gw5050 measured between PDMS-rubber surfaces at 0.1 Hz frequency of the rec drive.

It is also instructive to plot the friction force as a function of the normal load and extrapolate to zero normal load. This is done for the six glycerol/water mixtures measured between PDMS-rubber tribopairs for a rec drive frequency of 0.1 Hz (Figure A 11).

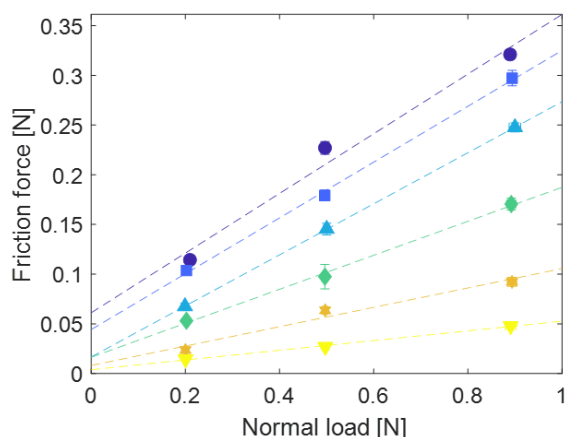


Figure A 11. Friction force versus normal load for glycerol/water mixtures of 50/50 (●), 60/40 (■), 70/30 (▲), 80/20 (◆), 90/10 (★) and 100/0 (▼) w/w% measured with PDMS-rubber tribopairs . Error bars indicate the standard deviation. The dotted lines are linear fits through each three data points belonging to one sample.

In this plot, the friction force decreases with viscosity of the sample. This is because with each higher viscosity, the lubrication is further down the mixed regime, where the friction decreases. Most noteworthy is that friction force would not equal zero when no normal load is applied (linear fits). This is possible if the probe and the substrate are still in touch (be it merely superficial) when the UMT TriboLab detects a normal load of 0 N. In fact, it was observed that this is indeed the case, see Figure A 18 in Appendix F.

APPENDIX E. LOAD VARIATIONS

During a measurement with UMT TriboLab, the applied load oscillates slightly around the set normal load force. The TriboLab tries to maintain the set normal load via a feedback loop that adjusts the carriage height (to which the probe holder is attached) such that load returns to the set force. Moving the carriage down pushes the probe harder on the substrate, increasing the load. The variations of the normal load and carriage height are in phase with the movement of the rec drive (i.e. with the position and velocity, which themselves oscillate with $\frac{1}{4}$ period phase difference with the same frequency), see Figure A 12a. Consequently, the variations in normal load and carriage height during a measurement step at a certain rec drive frequency can be plotted as a function of the position of the rec drive, giving a loop (Figure A 12b). Going around the loop once equals one oscillation of the rec drive. The normal load and the carriage height depend on both the position and the velocity of the rec drive, as the asymmetry in position and hysteresis with velocity of the curves show.

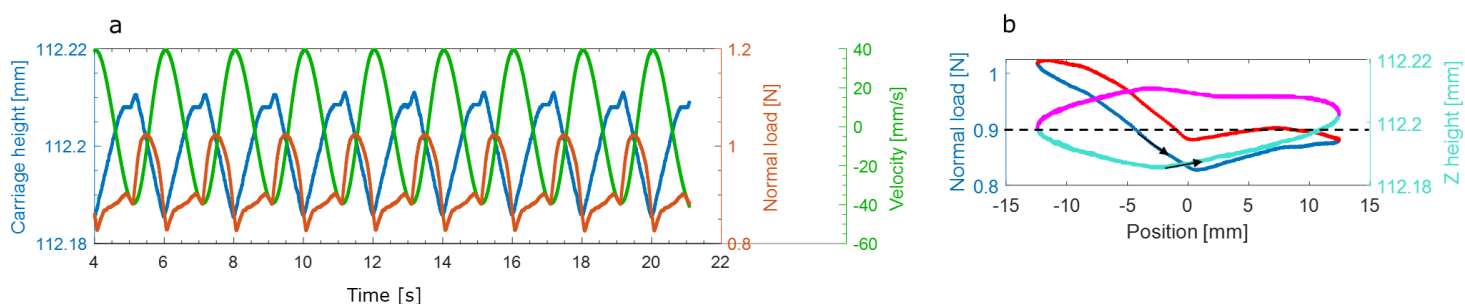


Figure A 12. (a) Oscillations in the velocity, normal load and carriage height with time during a measurement step with a rec drive frequency of 0.5 Hz and a set normal load of 0.9 N and (b) a plot of the normal load and carriage height in this step as a function of the position of the rec drive. In (b), (→) and (←) correspond to positive velocities, and (→) and (←) to negative. The arrows indicate the direction of movement over the loop. The dashed line indicates the set force. An increasing value of the Carriage / Z height means that the carriage (with the ball holder) moves down. Both graphs were obtained from a measurement with gw9010 with PDMS-rubber tribopairs.

The shape of the load versus position curves is influenced by the 'shape' of the substrate. This was in particular observed for the glass substrate. In all glycerol/water measurements, roughly two shapes of the load versus position curve emerged, corresponding to the two possible orientations of the glass plate (Figure A 13). For measurements on a rubber substrate, a wider variety of curve shapes was observed, which can be ascribed to the fact that many different rubber substrates are used across all measurements. However, curves with a higher force at the negative positions (as in Figure A 12b) were predominantly observed. This might point to the presence of a minimal slope in the rec drive.

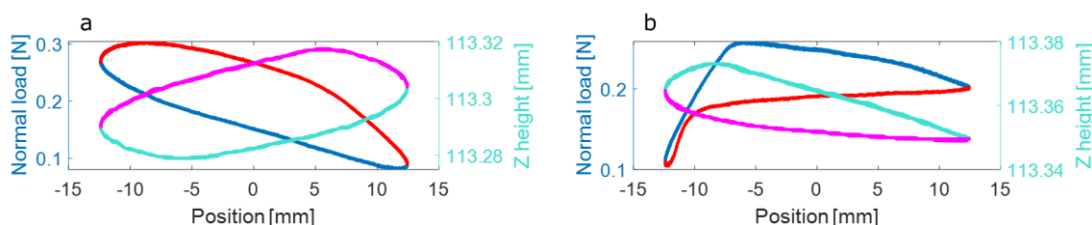


Figure A 13. Normal load and carriage (Z) height versus position of the rec drive for two orientations of the glass plate substrate in the rec drive. (→) and (←) correspond to positive velocities, and (→) and (←) to negative. The graphs were obtained from measurements with gw7030 (a) and gw6040 (b) with steel-glass tribopairs.

Across measurements, the magnitude of the fluctuations in normal load varies. The variation in normal load correlates with the variation in carriage height within a measurement step at a certain rec drive frequency (Figure A 14). This holds for different set normal loads and tribopairs. It might imply that variations in the normal load are at least partly related to the height profile / variations in the thickness of a substrate.

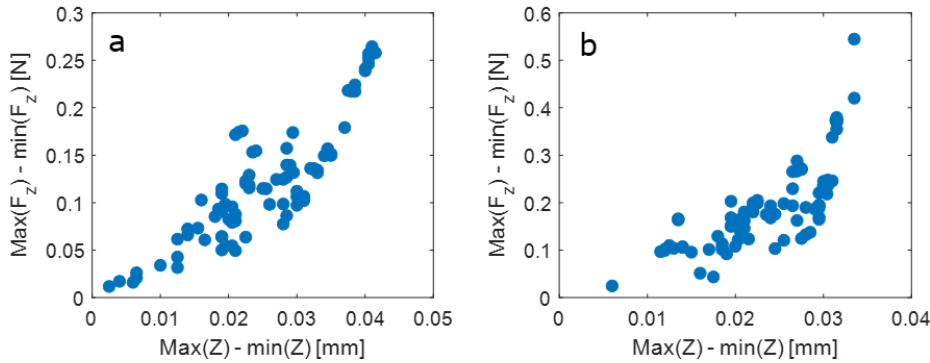


Figure A 14. Correlation between variations in normal load (F_z) and carriage height (Z) expressed as the maximum difference in each of these quantities during a measurement step at 0.5 Hz rec drive frequency at a set load of 0.2 N (a) and 0.9 N (b). Data of measurements with glycerol/water mixtures and sunflower oil with different tribopairs is used.

The variation in the magnitude of the fluctuations in normal load was further inspected by splitting the data out in different rec drive frequencies, set normal loads and tribopairs. Again, the maximum difference in normal load during a certain measurement step is used as a measure for the magnitude of the fluctuations. Figure A 15 presents histograms that show the distribution of the magnitude of the normal load variations across measurements under different measurement conditions. As an aid to the visual representation of the histograms, the fraction of data points in the 0-0.15 $\text{Max}(F_z) - \text{Min}(F_z)$ bins is displayed in each histogram. The larger this number, the lower the magnitude of the variations in normal load. In Figure A 15a, measurements are grouped per rec drive frequency, where 0.1 Hz is the lowest frequency used in all tribological measurements and the other frequencies are the subsequent steps. It is clear that with increasing frequency, the fluctuations in normal load increase for the first three steps. At lower speed, the carriage has more time to respond to small variations in the substrate height and to adjust its position such that the deviations from the set normal load remain limited. There is no difference observed anymore between the steps of 0.5 Hz and 0.75 Hz. Figure A 15b demonstrates that the magnitude of the normal load fluctuations increases with the set normal load. Perhaps, when the carriage pushes harder on the substrate, the impact of a small height variation in the substrate is larger. Thirdly, in Figure A 15c it is shown that the variations in normal load increase with the stiffness of the tribopair materials (section 3.2.2 informs on the stiffnesses). A justification for this could be that a material that is more easily deformed, has a larger capacity to absorb part of the variation in normal load (that is potentially induced by a change in the carriage height).

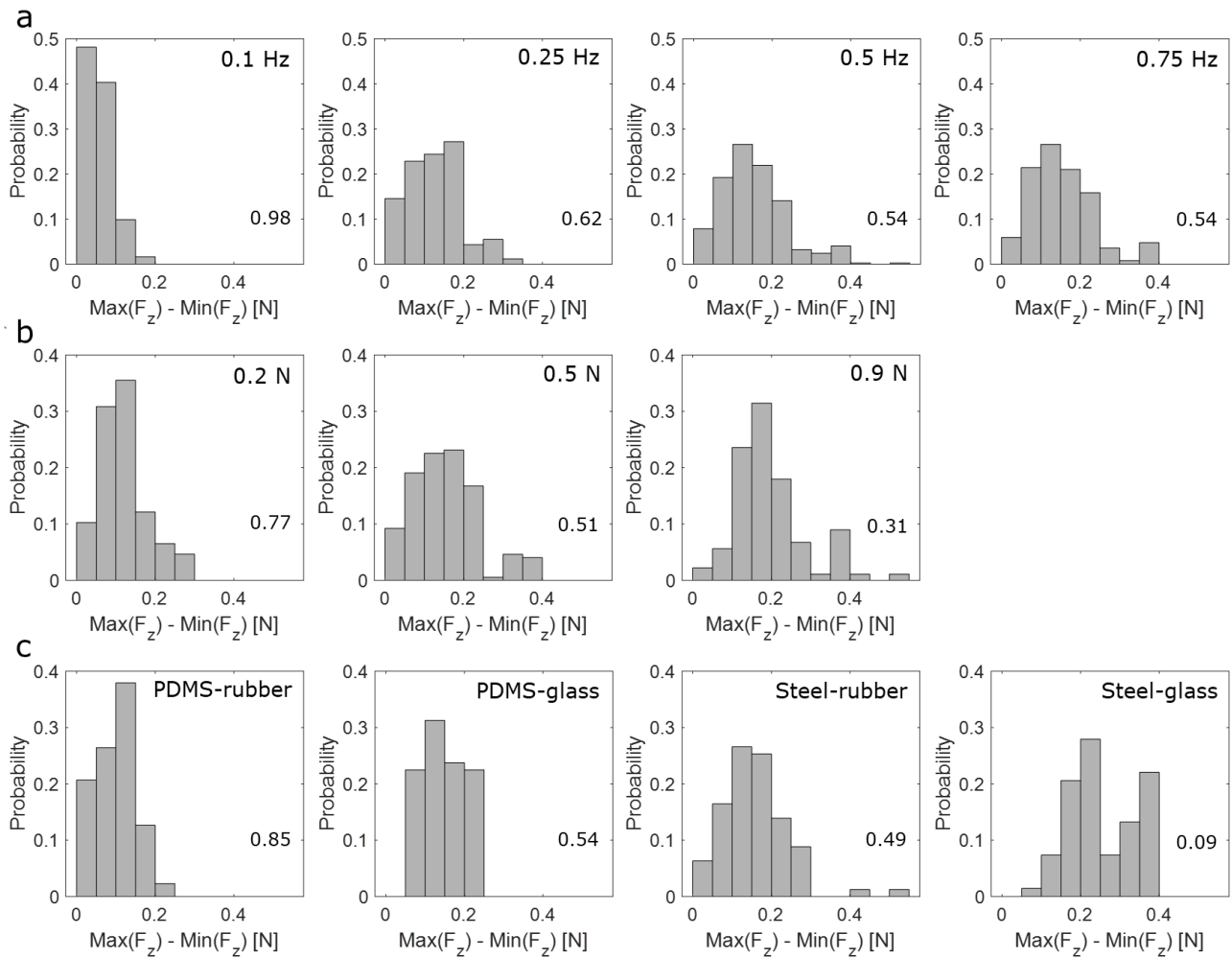


Figure A 15. Histograms showing the variation in normal load F_z (in terms of the maximum difference in normal load within a measurement step) across different measurement conditions: (a) frequency of the rec drive, (b) set normal load, (c) tribopair materials. Data in (b) and (c) is collected at a rec drive frequency of 0.5 Hz. The numbers displayed at the right bottom of the histograms are the fractions of data points in the $0 - 0.15 \text{ Max}(F_z) - \text{Min}(F_z)$ bins. The larger this number, the lower the fluctuations in normal load. All data is from measurements with glycerol/water mixtures and sunflower oil. In (a) at least 240 measurements are used, in (b) at least 90 and in (c) at least 70.

As a final point of importance, one might ask whether the fluctuations in the normal load would significantly affect the measured friction. Comparison of the friction curves of multiple measurements of the same sample (Figure A 16a, b) with curves of the corresponding normal loads at each speed (Figure A 16c) can shed some light on this. For this purpose, data with a relatively large spread in CoF vs speed curves among different measurements was used. No correlation can be observed between the order of the friction curves (which one has the highest and which one the lowest CoFs / friction forces) and the order of the normal load curves. It is more likely that small differences in the surface (structure and/or chemistry) of the substrates and probes contribute to differences in CoF versus speed curves between different measurements.

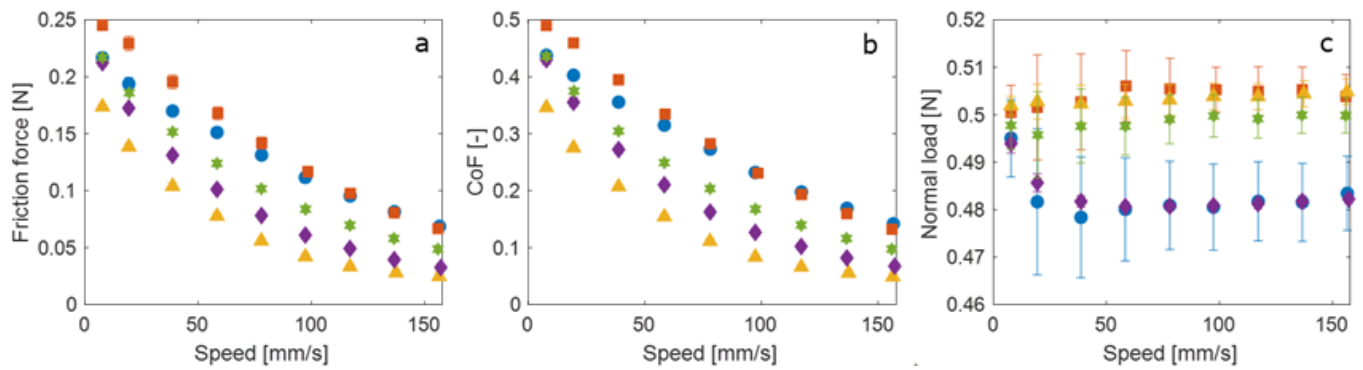


Figure A 16. Friction force (a) and CoF (b) versus speed curves of tribological measurements of gw5050 with PDMS-rubber tribopairs at 0.5 N normal load. (c) Average normal loads at the point where the friction force of each step is determined (at the maximum speeds). (●), (■) and (▲) were measured on different substrates. (◆) and (★) were measured at different positions on the same substrate. Error bars indicate standard deviation.

APPENDIX F. CONTACT AREA MEASUREMENTS

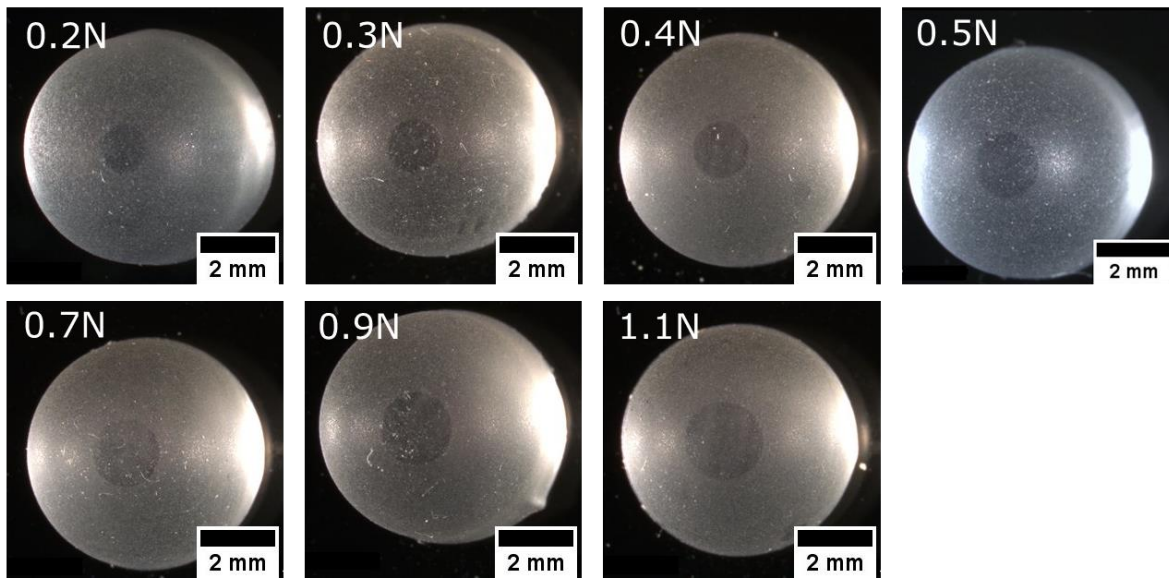


Figure A 17. Representative stereomicroscopy images of wear spots on PDMS probes used for the determination of the contact area between a PDMS probe and a rubber substrate in measurements with gw6040 as lubricant and at the normal loads reported in the images. The size of the wear spots was measured using ImageJ.



Figure A 18. Image of the ball holder with a PDMS probe after a tribological measurement on a rubber substrate at 0 N. There is a wear spot present on the probe. Before the measurement, the probe was brought in touch with the substrate with 0.08 N normal load, and then the UMT TriboLab retracted the probe until it measured a load of 0 N.

APPENDIX G. GLASS MICROSPHERES

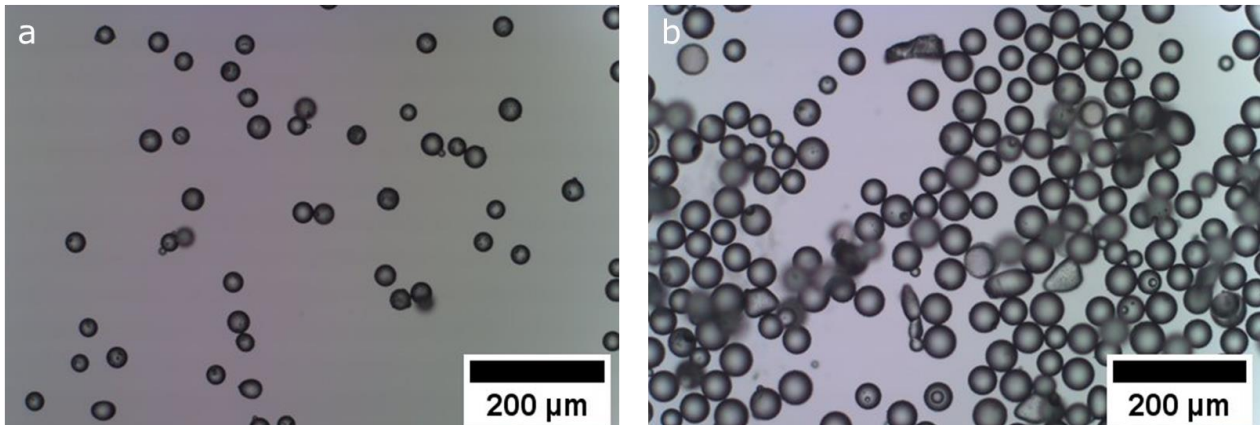


Figure A 19. Microscopy images of glass microspheres of (a) 20-30 μm and (b) 45-53 μm in diameter as stated by the supplier.

APPENDIX H. ROUGH SUBSTRATES

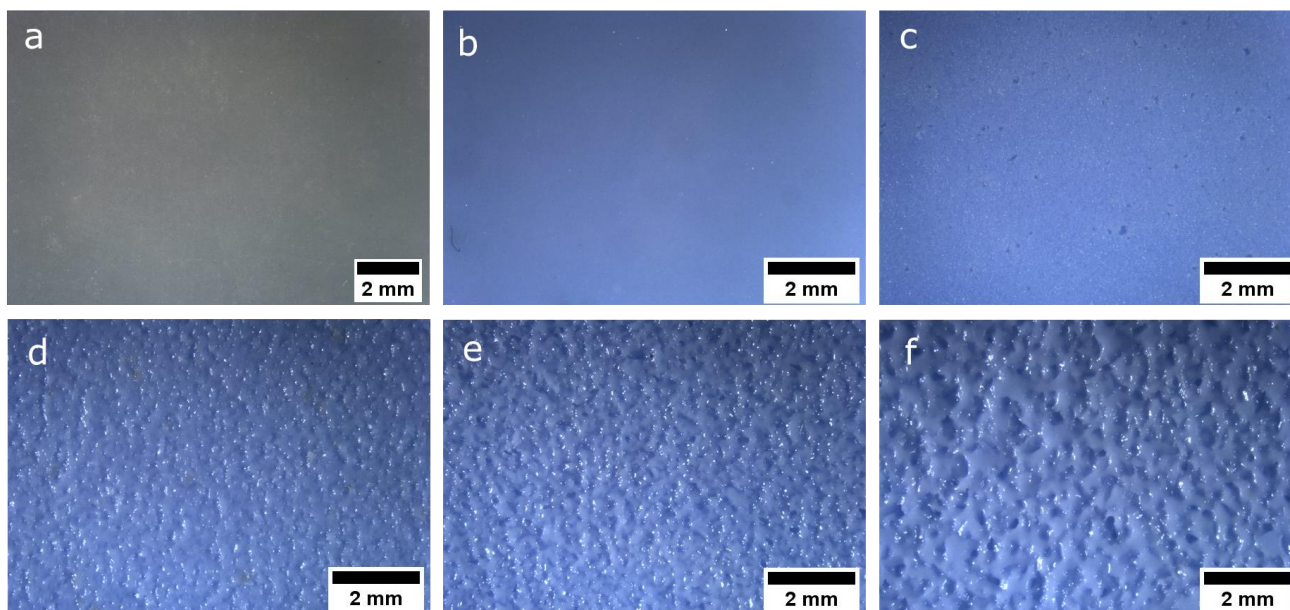


Figure A 20. Stereomicroscopy images of (a) a standard silicone substrate (shown as smooth reference) and substrates of different roughness fabricated by molding rubber putty on (b) a petri dish (smooth) and on sandpaper with grit size (c) P400, (d) P180, (e) P120 and (f) P80. Grit sizes correspond to average particle diameters of $201\ \mu\text{m}$ (P80), $125\ \mu\text{m}$ (P120), $82\ \mu\text{m}$ (P180) and $35\ \mu\text{m}$ (P400).⁴⁸

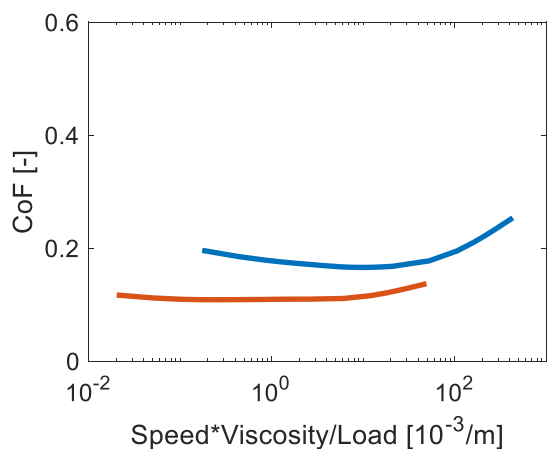


Figure A 21. Stribeck curves of glycerol/water mixtures measured with a PDMS probe on a P80 rough substrate at $0.5\ \text{N}$ (—) and $4\ \text{N}$ (—). $4\ \text{N}$ is the highest normal load the tribometer can apply without crossing the load detection limits during a measurement. The curves in are constructed using data of measurements with gw6040, gw8020 and glycerol.

APPENDIX I. VISCOSITY OF MILK, SALIVA AND ASTRINGENT MIXTURES

Table A 1. Viscosity of several milk, saliva and astringent mixtures. These values were used for the calculation of Stribeck curves. The viscosities of sm-lys and sm-tan could not be measured due to inhomogeneity of the samples (presence of protein aggregates). Abbreviations are as described in section 2.2.

Sample	Viscosity (mPas)
Salt solution	0.953
S-lys	1.011
S-tan	1.004
Salivam	4.726
Sm-lys	-
Sm-tan	-
Mfat0-s-lys	1.653
Mfat0-s-tan	1.654
Mfat0-sm-lys	1.836
Mfat0-sm-tan	1.815

APPENDIX J. ADDITIONAL STRIBECK CURVES MILK / SALIVA

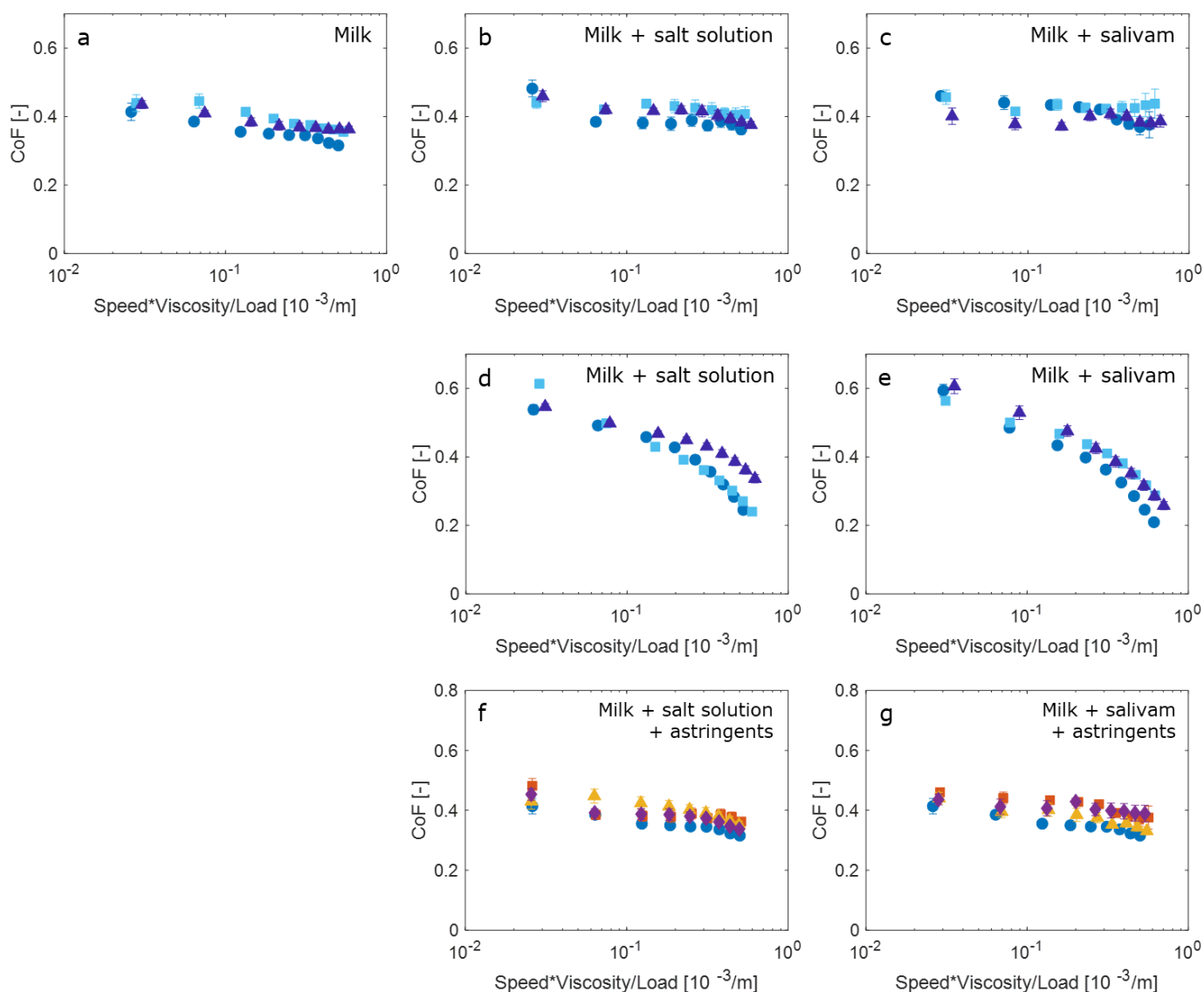


Figure A 22. Stribeck curves of milk, saliva and astringent mixtures measured at 0.5 N with steel-glass (a-c, f-g) tribopairs or PDMS-rubber (d, e) tribopairs. (a-e) ● = mfat0, ■ = mfat50 and ▲ = mfat100, optionally with salt solution or salivam added as stated in each figure. (f) Mfat0 (●), mfat0-s (■), mfat0-s-lys (▲), mfat0-s-tan (◆). (g) Mfat0 (●), mfat0-sm (■), mfat0-sm-lys (▲), mfat0-sm-tan (◆). Note that CoFs measured with steel-glass hardly depend on the speed, while CoFs measured with PDMS-rubber do so.

APPENDIX K. ADDITIONAL FRICTION CURVES SALIVA

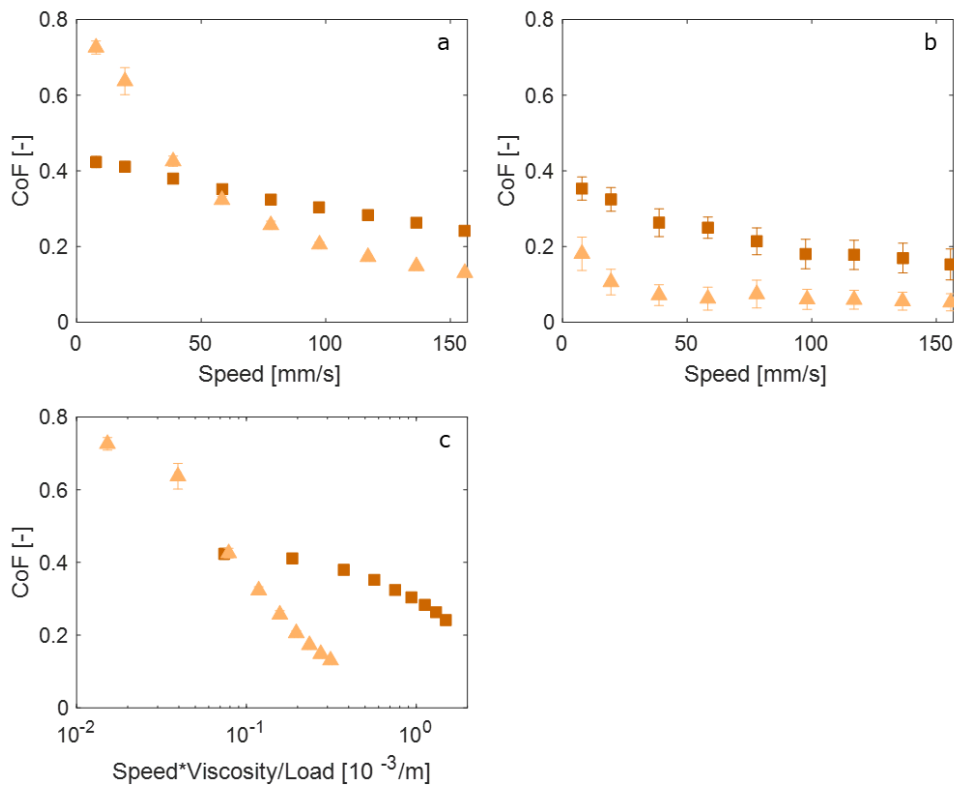


Figure A 23. CoF versus speed or speed*viscosity/load of salivam (■) and salt solution (▲) measured at 0.5 N between PDMS-rubber (a, c) and steel-glass (b) tribopairs. Error bars indicate standard deviation.